Electronic Supporting Information

Tuning the phototherapeutic activity of Pt(IV) complexes for bladder cancer via modification of *trans N*-heterocyclic ligands

Huayun Shi,[*a] Guy J. Clarkson,[a] Peter J Sadler[*a]

[a] Department of Chemistry, University of Warwick, Coventry CV4 7AL, UK.

Contents

Experimental Section

Materials and Instruments. 1-Methyl-5-nitroimidazole (**L2**) was purchased from ABCR, nicotinamide (**L3**) was purchased from Fluka, K_2PtCl_4, NaN_3, H_2O_2 (30%), 3-nitropyridine (**L1**), 4-methoxypyridine (**L4**), 3-fluoropyridine (**L5**), 3,5-difluoropyridine (**L6**) and other chemicals were from Sigma Aldrich and used without further purification.

NMR spectra were recorded on a Bruker Avance III HD 400 MHz or 500 MHz spectrometer using residual signal of the solvent as a reference. ESI-MS spectra were recorded on an Agilent 6130B single quadrupole detector instrument at 298 K with a scan range of m/z 50−2000 for positive ions and HR-ESI-MS data were collected on a Bruker microTOF instrument at 298 K. Electronic absorption spectra were recorded on a Varian Cary 300 UV-vis spectrophotometer in a quartz cuvette and solvent used as reference. The spectral width was 200–600 nm and the bandwidth was 1.0 nm, the scan rate was set to 600 nm/min. HPLC was carried out on an Agilent 1100 HPLC with an Agilent ZORBAX Eclipse XDB-C18 column (250×4.6 mm, 5 µm, flow rate: 1 mL/min), using linear gradients of 0.1% TFA in H_2O (solvent A) and 0.1% TFA in CH_3CN (solvent B). LC-MS was carried out on Bruker Amazon X mass spectrometry connected online to an Agilent 1260 HPLC with an Agilent ZORBAX Eclipse XDB-C18 column (250×4.6 mm, 5 µm, flow rate: 1 mL/min), using linear gradients of 0.1% FA in H_2O (solvent A) and 0.1% FA in CH_3CN (solvent B). The light sources used for photoactivation were LED light sources (BASETech model no. SP-GU10 230 V~50 Hz 1.3-2.1 W) with λ_{max} = 463 or 517 nm. A 96-array of LEDs with λ_{max} = 465 (4.8 mW cm^{-2} per LED) or 520 (11.7 mW cm^{-2} per LED) nm was used for *in vitro* growth inhibition. Whitley miniMACS Anaerobic Workstation equipped with a BOC gas cylinder (1% O_2/5% CO_2/94% N_2, 200 bar) was used to provide hypoxia environment for *in vitro* growth inhibition. Platinum contents were analysed on an ICP-MS 7900 (Agilent), ICP-OES 5300DV (Perkin Elmer) or ICP-OES 5800 (Agilent). The emission wavelength detected for Pt in ICP-OES was 265.945 nm.

Synthesis and characterisation. *Caution!* Even though we encountered no problem during this work, due care and attention with appropriate precautions should be taken in the synthesis and handling of shock-sensitive heavy metal azides in the dark.

Complex 1. A solution of K_2PtCl_4 (200 mg, 482 µmol) and 8 mol equiv. of 3-nitropyridine (478 mg, 3855 µmol) in 2 mL H_2O was stirred at 363 K for 24 h. To the resulting mixture, 20 mol equiv. of NaN_3 (628 mg, 9662 µmol) in 4 mL H_2O was added dropwise, and allowed stirring for another 24 h. The yellow precipitate (236 mg) was filtered, washed with H_2O and then EtOH, which was suspended in 20 mL H_2O_2, stirred at 318 K for 48 h giving yellow solution. The solution was filtered and lyophilized by freeze drying, then purified by column chromatography on silica gel (6% methanol + 94% DCM). Yield: 94 mg, 34%. HPLC purity: 99.3%. ^{1}H NMR (MeOD-d_4, 400 MHz): 9.92 (s with ^{195}Pt satellites, J^{195}Pt-^{1}H = 31.78 Hz, 2H, H_a), 9.40 (d with ^{195}Pt satellites, J = 5.83, J^{195}Pt-^{1}H = 27.36 Hz, 2H, H_d), 9.15 (d, J = 8.51, 2H, H_b), 8.16 (t, J = 6.55 Hz, 2H, H_c). ^{13}C NMR (MeOD-d_4, 125 MHz): 153.76 (*CH*), 145.72 (*C-NO$_2$*), 145.09 (*CH*), 136.77 (*CH*), 126.94 (*CH*). ESI-HR-MS: $[M + Na]^+$ (*m/z*) Calc., 584.0325; Found, 584.0320.

Complex 2. A solution of K_2PtCl_4 (200 mg, 482 µmol) and 6 mol equiv. of 1-methyl-5-nitroimidazole (**L2**, 376 mg, 2961 µmol) in 2 mL H_2O was stirred at 363 K for 24 h. To the resulting mixture, 20 mol equiv. of NaN_3 (628 mg, 9662 µmol) in 4 mL H_2O was added dropwise, and allowed stirring for another 24 h. The yellow precipitate (237 mg) was filtered, washed with H_2O and then EtOH, which was suspended in 20 mL H_2O_2, stirred at 318 K for 48 h giving a yellow solution. The solution was filtered and lyophilized by freeze drying, then purified by Biotage with Biotage® Sfär C18 D column. Yield: 58 mg, 21%. HPLC purity: 100%.^{1}H NMR (DMSO-d_6, 400 MHz): 9.00 (s with ^{195}Pt satellites, J^{195}Pt-^{1}H = 11.92 Hz, 2H,

H_a), 8.50 (d with ^{195}Pt satellites, J = 1.52 Hz, J^{195}Pt-^{1}H = 16.85 Hz, 2H, *H_b*), 4.17 (s, 6H, *CH_3*), 1.61 (s, 2H, *OH*). ^{13}C NMR (DMSO-*d_6*, 125 MHz): 140.16 (*CH*), 138.61 (*C-NO_2*), 127.36 (*CH*), 37.04 (*CH_3*). ESI-HR-MS: [M + Na]$^+$ (*m/z*) Calc., 590.0542; Found, 590.0545.

Complex 3. A solution of K_2PtCl_4 (200 mg, 481 µmol) and 6 mol equiv. of nicotinamide (353 mg, 2961 µmol) in 2 mL H_2O was stirred at 363 K for 24 h. To the resulting mixture, 20 mol equiv. of NaN_3 (628 mg, 9662 µmol) in 4 mL H_2O was added dropwise, and allowed stirring for another 24 h. The yellow precipitate (246 mg) was filtered, washed with H_2O and then EtOH, which was suspended in 20 mL H_2O_2, stirred at 318 K for 48 h giving yellow solution. The solution was filtered and lyophilized by freeze drying, then purified by semi-preparative HPLC. Yield: 5 mg, 2%. HPLC purity: 100%. ^{1}H NMR (DMSO-*d_6*, 400 MHz): 9.51 (s with ^{195}Pt satellites, J^{195}Pt-^{1}H = 29.34 Hz, 2H, *H_a*), 9.20 (d with Pt satellites, J = 5.75 Hz, J^{195}Pt-^{1}H = 27.32 Hz, 2H, *H_d*), 8.66 (d, J = 7.62 Hz, 2H, *H_b*), 8.45 (s, 2H, *C(O)NH_2*), 8.00-7.96 (m, 4H, *H_c and C(O)NH_2*), 2.43 (s, 2H, *OH*). ^{13}C NMR (DMSO-*d_6*, 125 MHz): 164.70 (*C(O)NH_2*), 151.15 (*CH*), 149.38 (*CH*), 140.30 (*CH*), 132.51 (*C-C(O)NH_2*), 126.17 (*CH*). ESI-HR-MS: [M + Na]$^+$ (*m/z*) Calc., 580.0739; Found, 580.0746.

Complex 4. A solution of K_2PtCl_4 (200 mg, 481 µmol) and 8 mol equiv. of 4-methoxypyridine (420 mg, 3855 µmol) in 2 mL H_2O was stirred at 363 K for 24 h. To the resulting mixture, 20 mol equiv. of NaN_3 (628 mg, 9662 µmol) in 4 mL H_2O was added dropwise, and allowed stirring for another 24 h. The yellow precipitate (122 mg) was filtered, washed with H_2O and then EtOH, which was suspended in 20 mL H_2O_2, stirred at 318 K for 48 h giving yellow solution. The solution was filtered and lyophilized by freeze drying, then purified by Biotage with Biotage® Sfär C18 D column. Yield: 52 mg, 23%. HPLC purity: 99.0%. ^{1}H NMR (MeOD-*d_4*, 500 MHz): 8.75 (d with ^{195}Pt satellites, J = 7.3 Hz, J^{195}Pt-^{1}H = 22.57 Hz, 4H, *H_a*), 9.20 (d, J = 7.35 Hz, 4H, *H_b*), 4.08 (s, 6H, *OCH_3*). ^{13}C NMR (MeOD-*d_4*, 125 MHz): 169.46 (*C-OCH_3*), 149.77 (*CH*), 111.72 (*CH*), 55.97 (*OCH_3*). ESI-HR-MS: [M + Na]$^+$ (*m/z*) Calc., 554.0835; Found, 554.0830.

Complex 5. A solution of K_2PtCl_4 (200 mg, 481 µmol) and 8 mol equiv. of 3-fluoropyridine (374 mg, 3856 µmol) in 2 mL H_2O was stirred at 363 K for 24 h. To the resulting mixture, 20 mol equiv. of NaN_3 (628 mg, 9662 µmol) in 4 mL H_2O was added dropwise, and allowed stirring for another 24 h. The yellow precipitate (203 mg) was filtered, washed with H_2O and then EtOH, which was suspended in 20 mL H_2O_2, stirred at 318 K for 48 h giving yellow solution. The solution was filtered and lyophilized by freeze drying, then purified by Biotage with Biotage® Sfär C18 D column. Yield: 49 mg, 20%. HPLC purity: 98.6%. ^{1}H NMR (MeOD-*d_4*, 500 MHz): 9.03 (t with ^{195}Pt satellites, J = 3.10 Hz, J^{195}Pt-^{1}H = 31.32 Hz, 2H, *H_a*), 8.95 (d with Pt satellites, J = 5.89 Hz, J^{195}Pt-^{1}H = 27.81 Hz, 2H, *H_d*), 8.21 (t, J = 8.04 Hz, J = 1.89 Hz, 2H, *H_b*), 7.94-7.88 (m, 2H, *H_c*). ^{13}C NMR (MeOD-*d_4*, 125 MHz): 158.45 (d, *C-F*), 145.94 (*CH*), 138.06 (d, *CH*), 129.07 (d, *CH*), 127.17 (d, *CH*). ESI-HR-MS: [M + Na]$^+$ (*m/z*) Calc., 530.0435; Found, 530.0430.

Complex 6. A solution of K_2PtCl_4 (200 mg, 481 µmol) and 8 mol equiv. of 3,5-difluoropyridine (444 mg, 3856 µmol) in 2 mL H_2O was stirred at 363 K for 24 h. To the resulting mixture, 20 mol equiv. of NaN_3 (628 mg, 9662 µmol) in 4 mL H_2O was added dropwise, and allowed stirring for another 24 h. The brown precipitate (125 mg) was filtered, washed with H_2O and then EtOH, which was suspended in 20 mL H_2O_2, stirred at 318 K for 48 h giving yellow solution. The solution was filtered and lyophilized by freeze drying, then purified by by column chromatography on silica gel (3% methanol + 97% DCM). Yield: 49 mg, 20%. HPLC purity: 99.4%. ^{1}H NMR (MeOD-*d_4*, 500 MHz): 8.99 (t with ^{195}Pt satellites, J = 1.74 Hz, J^{195}Pt-^{1}H = 32.48 Hz, 4H, *H_a*), 8.38 (tt, J_1 = 8.19 Hz, J_2 = 2.41 Hz, 2H, *H_b*). ^{13}C NMR (MeOD-*d_4*, 125 MHz): 159.51 (dd, *C-F*), 135.23 (d, *CH*), 118.14 (d, *CH*). ESI-HR-MS: [M + Na]$^+$ (*m/z*) Calc.,

566.0246; Found, 566.0245.

X-Ray crystallography. Single crystals of **1**−**6** were grown by evaporation of their methanol solution. A suitable crystal was selected and mounted on a glass fibre with Fomblin oil and placed on a Rigaku Oxford Diffraction SuperNova diffractometer with a dual source (Cu at zero) equipped with an AtlasS2 CCD area detector. The crystal was kept at 150(2) K during data collection. Using Olex2[1], the structure was solved with the ShelXT[2] structure solution program using Intrinsic Phasing and refined with the ShelXL[3] refinement package using Least Squares minimisation. CCDC 2359629, 2359630, 2360200, 2360222, 2360223 and 2360225 contain the supplementary crystallographic data for this paper.

Electrochemistry. All cyclic voltammogram (CV) experiments were carried out using a CH Instrument model 600D Electrochemical Analyzer/Workstation (Austin, TX). The complex (1 mM) solution was prepared in acetonitrile containing tetrabutylammonium hexafluorophosphate (0.1 M) as supporting electrolyte and degassed under nitrogen. A typical three-electrode system was used to scan the cyclic voltammograms: a glassy carbon electrode as the working electrode, $Ag/AgNO_3$ (10 mM in acetonitrile) as the reference electrode, and platinum wire as the counter electrode. The scan rate was 100 mV/s.

Dark stability and photoactivation in solution. The dark stability and photoactivation of complexes (OD_{300} = 1) in air- or N_2-saturated PBS with 5% v/v DMSO in the presence of 2 mM GSH was monitored by UV-vis spectroscopy. The photoactivation of the complexes alone in air- or N_2-saturated MilliQ water with 5% v/v DMSO was also monitored by UV-vis. The dark stability in aqueous solution was monitored by LC-MS at different time intervals alone, or in the presence of 2 mM GSH at 310 K. The photoactivation in aqueous solution was also determined by LC-MS at different time intervals upon irradiation with blue (463 nm) and green (517 nm) light at 298 K.

Liver microsomal stability. Complex (100 μM) was incubated with liver microsomes and NADPH at 310 K in the dark for 24 h in both air- and N_2-saturated PBS solution for 24 h. 750 μL acetonitrile was added to the 750 μL solution to precipitate proteins, then centrifuged at 13500 RPM for 30 min. Collect the solutions and freeze dry them. 750 μL MilliQ water was added to redissolve platinum species. The solution was filtered through a syringe filter before injection into LC-MS.

Electron paramagnetic resonance (EPR) spectroscopy. The EPR spectra were recorded on a Bruker EMX (X-band) spectrometer at 298 K. Samples (*ca*. 100 μL) in aqueous solution were prepared and transferred using a plastic syringe with metal needle to a standard quality quartz tube with inner diameter of 1.0 mm and outer diameter of 2.0 mm (Wilmad LabGlass) and sealed with parafilm. Using the y-incremental sweep mode of 100 with an accumulation of 5 scans in the x dimension. Typical key EPR spectrometer settings were modulation amplitude 1.0 G, microwave power 6.31 mW, receiver gain 1.0×10^5, conversion time 10.24 ms, time constant 10.24 ms, sweep width 200 G. The blue LED (463 nm) fitted into a GU-10 device was mounted within the EPR magnet, supported by a foam sponge, to maintain its position throughout the EPR measurements. The distance from the tip of the irradiation light bulb to the EPR cavity was *ca*. 5 cm. Data were processed by Matlab R2021b with easyspin 5.2.35.

Photoreaction with 5'-GMP. 2 mol. equiv. of guanosine 5′-monophosphate disodium salt hydrate (5′-GMP-Na_2) was mixed with 50 μM complex in aqueous solution. The solution was irradiated for 1 h (463 nm) and analysed immediately on a Bruker Amazon X mass spectrometer connected online with HPLC.

Cell culture. Human cell lines, ovarian carcinoma A2780 and cisplatin-resistant A2780cis cells, and lung fibroblast MRC-5 cell, were obtained from the European Collection of Animal Cell Culture (ECACC), Salisbury, UK. Bladder cancer SW-780 and VM-CUB-1 cells were provided by Dr Richard T. Bryan from (University of Birmingham). Normal bladder epithelial SV-HUC-1 cells were obtained from CLS Cell Lines Service GmbH. SV-HUC-1 cells were grown in Kaighn's Modification of Ham's F-12 Medium (F-12K Medium), while other cell lines used in this work were grown in Roswell Park Memorial Institute media (RPMI-1640). All media were supplemented with 10% v/v of foetal calf serum (FCS) and 1% v/v penicillin/streptomycin. The adherent monolayers of cells were grown at 310 K in a humidified atmosphere containing 5% CO_2 and passaged regularly at *ca*. 80% confluence.

Photo-dark cytotoxicity under normoxia and hypoxia. Approximately 1×10^4 cells were seeded per well in 96-well plates. Independent duplicate plates were used, one for dark while the other for irradiation experiment. The cells were pre-incubated in drug-free medium with phenol red at 310 K for 24 h. For normoxia experiments, drugs were added after pre-incubation, while for hypoxia experiments, plates were transferred to hypoxia chamber and allowed another 24 h incubation under hypoxia environment, and all the remaining experiments were carried out under hypoxia. Drug treatments under these two conditions were exactly same except for the oxygen concentration. Complexes were dissolved first in DMSO and then diluted in phenol red-free medium to make the stock solution of the drug. These stock solutions were further diluted using phenol-red free cell culture medium until working concentrations were achieved with DMSO concentration adjusted to be 0.05% v/v in these solutions. Cells were exposed to the drugs with different concentrations for 1 h. One plate was irradiated for 1 h using blue light (4.8 mW cm^{-2} per LED at 465 nm) or green light (11.7 mW cm^{-2} per LED at 520 nm), while the dark plate was kept in the incubator. After irradiation, cells were incubated for another 72 h at 310 K under corresponding oxygen concentration without drug removal. Untreated controls that were only exposed to vehicle were also compared between the irradiated and the non-irradiated plates to ensure that the differences in cell survival were not statistically relevant, hence guaranteeing that the differences in cell viability observed were not due to the light source. The SRB assay was used to determine cell viability.[4] Absorbance measurements of the solubilised dye (on a Tecan microplate reader) allowed the determination of viable treated cells compared to untreated controls. IC_{50} values (concentrations which caused 50% of cell death) were determined as the average of triplicates and their standard deviations were calculated. Stock concentrations for all metal complexes used in these biological assays were adjusted/verified after ICP-OES metal quantification.

Extraction of platinum compounds from cell culture medium. SW780 cells (*ca*. 5×10^5) were seeded in 6-well plates and cultured 24 h for attachment. Half of the plates were moved to hypoxia chambers and left for 24 h and all the remaining experiments were carried out under hypoxia. Drug treatments under these two conditions are exactly same except for the oxygen concentration. Cells were incubated with complexes at 20 μM in phenol red-free medium with 0.05% v/v DMSO for 2 h in the dark or 1 h in the dark then 1 h upon irradiation (465 nm or 520 nm). 1 mL acetonitrile was added to the 1 mL supernatant collected to precipitate proteins, then centrifuged at 13500 RPM for 30 min. The collected solutions freeze-dried. 0.5 mL MilliQ water was added to each sample to redissolve platinum species. The solution was filtered through a syringe filter before injection into LC-MS.

Platinum accumulation in cancer cells. For Pt cellular accumulation studies, *ca*. 5×10^6 A2780, A2780cis and SW780 cells were plated in 100 mm Petri dishes and allowed to attach for 24 h. For normoxia experiments, drugs were added after pre-incubation, while for hypoxia experiments, plates were transferred to hypoxia chamber and allowed another 24 h incubation under hypoxia environment, and the remaining of the experiments were carried out under

hypoxia. Drug treatments under these two conditions are exactly same except for the oxygen concentration. The plates were exposed to complexes at 10 μM in phenol red-free medium with 0.05% v/v DMSO. Additional plates were incubated with vehicle alone as a negative control. After 1 h of incubation in the dark at 310 K, one plate was left in the dark for another 1 h in the incubator, while the other one was irradiated with blue light (4.8 mW cm^{-2} per LED at 465 nm) or green light (11.7 mW cm^{-2} per LED at 520 nm). The cells were rinsed three times with cold PBS and harvested by trypsinisation. The number of cells in each sample was counted manually using a haemocytometer. Then the cells were centrifuged to obtain the whole cell pellet for ICP-MS analysis. All experiments were conducted in triplicate.

Intracellular distribution. *ca*. 1×10^7 SW780 cells were plated in Petri dishes and allowed to attach for 24 h. For normoxia experiments, drugs were added after pre-incubation, while for hypoxia experiments, plates were transferred to hypoxia chamber and allowed another 24 h incubation under hypoxia environment, and all the remaining experiments were carried out under hypoxia. Drug treatments under these two conditions are exactly same except for the oxygen concentration. Then the plates were exposed to complexes at 10 μM in the dark for 2 h at 310 K. Cells were rinsed three times with cold PBS and harvested by trypsinisation. The number of cells in each sample was counted manually using a haemocytometer. Mitochondria/Cytosol Fractionation Kit (Sigma Aldrich) was used to extract nuclei, mitochondria and cytoplasm. All experiments were conducted in duplicate.

Platinum accumulation in rat bladder. All *ex vivo* experiments were carried out in BSU at University of Warwick and approved by the University of Warwick's Animal Welfare and Ethical Review Body (AWERB). No Home Office ASPA Project Licence is required for this work. Fresh bladders were removed from female Sprague–Dawley® rats (8-10 weeks old) and washed with PBS. Bladders were cut and flattened, with the inner layer is upwards. The bladder was weighed and incubated with 50 μM complex in PBS with 0.05% DMSO in the dark for 1 h at 310 K. One bladder was irradiated with blue light (4.8 mW cm^{-2} per LED at 465 nm) for 1 h, while the other one was left in the incubator. The bladders were rinsed with PBS twice. All experiments were conducted in triplicate.

ICP-MS sample preparation. Cell pellet: whole cell pellets in Eppendorf tubes were dissolved in concentrated 72% v/v nitric acid (200 μL), and heated in an oven at 343 K overnight. The samples were then allowed to cool, and each cellular sample solution was transferred into a Falcon tube and diluted with Milli-Q water (3.8 mL), to obtain a final HNO_3 concentration of *ca*. 3.6% v/v. **Rat bladder**: the bladders in Falcon tubes were dissolved in concentrated 72% v/v nitric acid (1000 μL), and heated in an oven at 343 K overnight. The samples were then allowed to cool, and 300 μL of each rat sample solution was transferred into another Falcon tube and diluted with Milli-Q water (5.7 mL), to obtain a final HNO_3 concentration of *ca*. 3.6% v/v.

Confocal Fluorescence Microscopy. The fluorescence images were recorded on a fluorescence confocal microscope (LSM 880, AxioObserver). SW780 cells (*ca*. 1×10^5) were seeded in glass bottom cell culture dishes (CELLview) and cultured 24 h for attachment. Half of dishes were moved to hypoxia chambers and left for 24 h and all the remaining experiments were carried out under hypoxia. Drug treatments under these two conditions were exactly same except for the oxygen concentration. **ROS generation.** Cells were exposed to complex in the absence and presence of NAC for 1 h in the dark then 1 h irradiation with blue light (465 nm). Drugs were removed and cells were incubated with DCFH-DA (20 μM) for 30 min. Cells were washed by HBSS before measurement. **Mitochondrial membrane potential.** Cells were exposed to complex for 1 h in the dark then 1 h irradiation with blue light (465 nm), then further incubated with drugs for 72 h after irradiation. Drugs were removed and cells were incubated

with TMRE (tetramethylrhodamine ethyl ester, 200 nM) for 30 min. Cells were washed by PBS before measurement.

Flow Cytometry. All flow cytometry experiments were carried out using a Becton Dickinson FACScan flow cytometer in the School of Life Sciences at University of Warwick. SW780 cells (*ca.* 5×10^5) were seeded in 6-well plates and cultured 24 h for attachment. Half of the plates were moved to hypoxia chambers and left for 24 h and all the remaining experiments were carried out under hypoxia. Drug treatments under these two conditions are exactly same except for the oxygen concentration. **Lipid peroxidation assay.** Cells were exposed to complex for 1 h in the dark then 1 h irradiation with blue light (465 nm). Drugs were removed and cells were incubated with BODIPY™ 581/591 C11 (5 μM) for 30 min. Cells were washed by HBSS before measurement. **Apoptosis assay.** Cells were exposed to complex for 1 h in the dark then 1 h irradiation with blue light (465 nm), and further incubated with drugs for 72 h after irradiation, then washed with PBS and treated with Annexin V-FITC/PI kit (Abcam). **Mitochondrial membrane potential.** Cells were exposed to complex for 1 h in the dark then 1 h irradiation with blue light (465 nm), and further incubated with drugs for 0, 24 or 72 h after irradiation. Drugs were removed and cells were incubated with TMRE (200 nM) for 30 min. Cells were washed by PBS before measurement.

Table S1. UV-vis absorption spectra of **1**, **2**, and **FM190** in water at 298 K.

Compound	λ_{abs}/nm (ε_{max}/$M^{-1}cm^{-1}$)
1	241 (16173); 275 (16109); 294 (16817)
2	289 (30007)
3	267 (14219); 295 (18100)
4	242 (30167); 292 (18159)
5	267 (15257); 296 (18699)
6	272 (18214); 299 (19839)
FM190[5]	259 (10721); 293 (17412)

Table S2. Crystallographic data and structure refinement for complexes **1** and **2**.

Complex	**1**	**2**
CCDC Code	2359629	2359630
Formula	$C_{10}H_{14}N_{10}O_8Pt$	$C_8H_{12}N_{12}O_6Pt$
$D_{calc.}$/ g cm^{-3}	2.307	2.355
m/mm^{-1}	15.922	17.003
Formula Weight	597.40	567.39
Colour	yellow	yellow
Shape	block-shaped	block-shaped
Size/mm^3	0.16×0.14×0.10	0.14×0.10×0.04
T/K	150(2)	150(2)
Crystal System	monoclinic	monoclinic
Space Group	$P2_1/c$	$C2/c$
a/Å	8.41391(5)	44.2587(3)
b/Å	8.47823(5)	6.43041(5)
c/Å	12.06815(7)	11.27230(8)
a/°	90	90

b/°	92.5019(5)	93.8974(6)
g/°	90	90
V/Å^3	860.062(9)	3200.70(4)
Z	2	8
Z'	0.5	1
Wavelength/Å	1.54184	1.54184
Radiation type	CuK$_a$	CuK$_a$
Q_{min}/°	5.262	4.005
Q_{max}/°	73.477	73.813
Measured Refl's.	25444	46426
Indep't Refl's	1737	3203
Refl's I≥2 *s*(I)	1729	3194
R_{int}	0.0326	0.0359
Parameters	145	249
Restraints	0	0
Largest Peak	0.841	0.702
Deepest Hole	-1.335	-0.911
GooF	1.163	1.222
wR_2 (all data)	0.0431	0.0379
wR_2	0.0430	0.0378
R_1 (all data)	0.0162	0.0155
R_1	0.0161	0.0154

Table S3. Crystallographic data and structure refinement for complexes **3**–**6**.

Complex	**3**	**4**	**5**	**6**
CCDC code	2360222	2360200	2360223	2360225
Empirical formula	$C_{12}H_{14}N_{10}O_4Pt$	$C_{14}H_{24}N_8O_6Pt$	$C_{10}H_{10}F_2N_8O_2Pt$	$C_{10}H_8F_4N_8O_2Pt$
Formula weight	557.42	595.50	507.35	543.33
Temperature/K	150(2)	100(2)	150(2)	150(2)
Crystal system	triclinic	monoclinic	triclinic	triclinic
Space group	P-1	$P2_1/n$	P-1	P-1
a/Å	8.66940(10)	7.49583(11)	8.5213(2)	8.20270(10)
b/Å	8.98250(10)	11.24240(14)	9.1386(2)	11.31510(10)
c/Å	12.0502(2)	12.31797(19)	9.4163(3)	24.5296(2)
α/°	69.5790(10)	90	87.630(2)	78.7960(10)
β/°	77.1920(10)	106.6288(15)	71.112(2)	88.7040(10)
γ/°	72.7180(10)	90	85.2375(19)	84.7870(10)
Volume/Å^3	832.37(2)	994.64(3)	691.32(3)	2224.04(4)
Z	2	2	2	6
ρ_{calc}g/cm^3	2.224	1.988	2.437	2.434
μ/mm^{-1}	16.203	13.650	19.468	18.423
F(000)	532.0	580.0	476.0	1524.0
Crystal size/mm^3	0.16 × 0.16 × 0.06 yellow block	0.277 × 0.205 × 0.026 yellow block	0.14 × 0.12 × 0.02 yellow block	0.18 × 0.18 × 0.08 yellow block
Radiation	Cu Kα (λ = 1.54184)	Cu Kα (λ = 1.54184)	Cu Kα (λ = 1.54184)	Cu Kα (λ = 1.54184)
2Θ range for data collection/°	7.898 to 147.286	10.868 to 160.114	9.714 to 147.664	7.348 to 147.26
Index ranges	-10 ≤ h ≤ 10, -11 ≤ k ≤ 11, -14 ≤ l ≤ 14	-9 ≤ h ≤ 9, -14 ≤ k ≤ 14, -15 ≤ l ≤ 14	-10 ≤ h ≤ 10, -11 ≤ k ≤ 11, -11 ≤ l ≤ 11	-10 ≤ h ≤ 9, -14 ≤ k ≤ 14, -30 ≤ l ≤ 30

Reflections collected	41394	28170	39688	106492
Independent reflections	3174 [R_{int} = 0.0885, R_{sigma} = 0.0256]	2145 [R_{int} = 0.1024, R_{sigma} = 0.0319]	2780 [R_{int} = 0.0632, R_{sigma} = 0.0181]	8926 [R(int) = 0.0701]
Data/restraints/parameters	3174/0/249	2145/1/139	2780/2/218	8926/0/704
Goodness-of-fit on F^2	1.128	1.162	1.073	1.318
Final R indexes [I>=2σ (I)]	R_1 = 0.0217, wR_2 = 0.0591	R_1 = 0.0304, wR_2 = 0.0877	R_1 = 0.0219, wR_2 = 0.0633	R_1 = 0.0220, wR_2 = 0.0556
Final R indexes [all data]	R_1 = 0.0222, wR_2 = 0.0595	R_1 = 0.0316, wR_2 = 0.0891	R_1 = 0.0235, wR_2 = 0.0659	R_1 = 0.0220, wR_2 = 0.0556
Largest diff. peak/hole / e $Å^{-3}$	1.43/-1.91	1.44/-1.77	1.19/-1.66	1.34/-1.06

Table S4. Selected bond lengths (Å) and bond angles (°) for complexes **1** and **2**.

1		**2**	
Pt1–O1	2.013(3)	O1–Pt1	2.0085(18)
Pt1–N1	2.030(2)	Pt1–O2	2.002(2)
Pt1–N7	2.069(3)	N1–Pt1	2.018(2)
O1–Pt1–O1[1]	180.0	Pt1–N6	2.010(2)
N1–Pt1–N1[1]	180.00(8)	Pt1–N11	2.041(2)
N7[1]–Pt1–N7	180.00(12)	Pt1–N14	2.056(2)
N9–N8–N7	174.6(3)	O2–Pt1–O1	176.74(8)
N8–N7–Pt1	116.5(2)	N6–Pt1–N1	177.99(8)
O3B–N3–O3A	125.2(3)	N11–Pt1–N14	175.53(9)
		N13–N12–N11	173.4(3)
		N16–N15–N14	176.1(3)
		N12–N11–Pt1	119.95(19)
		N15–N14–Pt1	113.02(18)
		O4B–N4–O4A	125.0(2)
		O9B–N9–O9A	124.8(2)

[1]1-X,1-Y,1-Z

Table S5. Selected bond lengths (Å) and bond angles (°) for complexes **3**–**6**.

3		**4**	
Pt1–O1	2.0040(15)	Pt1–O1	2.0094(15)
Pt1–N101	2.0542(19)	Pt1–N3	2.046(5)
Pt1–N109	2.0567(18)	Pt1–N91	2.0518(19)
C107–O107	1.241(3)	O1–Pt1–O11	180.0
O12–Pt1–O1	180.0	N3–Pt1–N3[2]	180.0
N101–Pt1–N101[1]	180.0	N9[2]–Pt1–N9	180.0
N109[1]–Pt1–N109	180.00(10)	N11–N10–N9	175.0(2)
N110–N109–Pt1	114.69(15)	N10–N9–Pt1	115.28(15)
N101–C106–C105	122.0(2)		
N108–C107–C105	118.2(2)		
O107–C107–C105	119.1(2)		
5		**6**	
Pt1–O1	2.0033(17)	Pt1–O11A	2.018(3)
Pt1–N101	2.028(3)	Pt1–O11B	1.994(3)

Pt1–N107	2.049(2)	Pt1–N11A	2.022(3)
F103–C103	1.340(5)	Pt1–N11B	2.033(3)
N101–Pt1–N101[3]	180.00(16)	Pt1–N11C	2.044(3)
O1[3]–Pt1–O1	180.0	Pt1–N11D	2.064(3)
N107[3]–Pt1–N107	180.00(7)	O11B–Pt1–O11A	177.99(11)
N108–N107–Pt1	117.83(19)	N11A–Pt1–N11B	178.88(13)
N109–N108–N107	174.1(3)	N11C–Pt1–N11D	179.08(13)
		N12C–N11C–Pt1	114.7(3)
		N12D–N11D–Pt1	115.9(3)
		N13C–N12C–N11C	174.9(4)

[1]2-X,-Y,1-Z; [2]1-X,1-Y,-Z; [3]1-X,1-Y,2-Z;

Table S6. Selected hydrogen bonds parameters for complexes **1** and **2**.

Comp	D	H	A	d(D-H)/Å	d(H-A)/Å	d(D-A)/Å	D-H-A/°
1	O1	H1	O10[1]	0.84	2.04	2.805(3)	151.9
	O10	H10B	O1	0.87	1.80	2.658(4)	168.4
2	O1	H1	N14[2]	0.84	2.24	3.064(3)	165.0
	O2	H2A	N16[3]	0.84	2.34	3.146(3)	161.5
3	O2	H2	O107[4]	0.84	2.08	2.895(2)	164.6
	N108	H10A	O2	0.88	1.98	2.852(3)	172.5
	N108	H10B	N109[5]	0.88	2.33	3.185(3)	164.3
4	O100	H100	O1	0.84	1.89	2.723(3)	173.9
	O1	H1	O100[6]	0.847(19)	2.01(2)	2.854(3)	172(4)
5	O1	H1	N209[7]	0.83(2)	2.35(2)	3.170(3)	166(4)
	O2	H2	N109[8]	0.84(2)	2.40(2)	3.215(3)	164(4)
6	O11A	H11A	F23A[9]	0.84	2.68	3.431(4)	150.0
	O11B	H11B	N21C	0.84	2.23	3.018(4)	156.0
	O21A	H21A	N23D[10]	0.84	2.31	3.121(4)	164.1
	O21B	H21B	O11A[11]	0.84	2.07	2.865(4)	157.3
	O31	H31	O41[12]	0.84	2.15	2.853(6)	141.5
	O31	H31	O41A[12]	0.84	2.10	2.851(14)	148.7
	C12B	H12B	O21A	0.95	2.12	2.996(5)	153.2

[1]1-X,0.5+Y,1.5-Z; [2]+X,1-Y,1/2+Z; [3]+X,1+Y,+Z; [4]1-X,1-Y,-Z; [5]-1+X,+Y,+Z; [6]-X,1-Y,-Z; [7]1-X,1-Y,1-Z; [8]1-X,2-Y,1-Z; [9]-1+X,1+Y,+Z; [10]1-X,-Y,2-Z; [11]+X,-1+Y,+Z; [12]-1+X,+Y,+Z

Table S7. Mass and corresponding formulae of photoproducts from **1** (50 μM) determined by LC-MS (mobile phase: water and acetonitrile).

Peak	Retention time/min	Mass calculated	Mass observed	Formula
a	5.4	1073.08	1072.91	$[2\{Pt^{IV}(\mathbf{L1})_2(N_3)(OH)_3\}+H]^+$
b	8.1	584.03	583.96	$[\mathbf{1}+Na]^+$
c	9.1	125.04	124.97	$[\mathbf{L1}+H]^+$
d	12.0	526.06	525.93	$\{Pt^{II}(\mathbf{L1})_2(N_3)(CH_3CN)\}^+$
e	12.5	533.01	532.93	$\{Pt^{III}(\mathbf{L1})_2(HCOO)_2\}^+$

Table S8. Mass and corresponding formulae of photoproducts from **2** (50 μM) determined by LC-MS (mobile phase: water and acetonitrile).

Peak	Retention time/min	Mass calculated	Mass observed	Formula

a	4.2	1084.95	1084.95	$[2\{Pt^{IV}(\mathbf{L2})_2(N_3)(OH)_3\}+H]^+$
b	6.2	590.05	589.96	$[\mathbf{2}+Na]^+$
c	11.6	584.03	583.99	$\{Pt^{IV}(\mathbf{L2})_2(HCOO)_3\}^+$
d	12.9	532.08	531.97	$\{Pt^{II}(\mathbf{L2})_2(N_3)(CH_3CN)\}^+$
e	15.5	618.09	618.08	$\{Pt^{II}(\mathbf{L2})_3(N_3)\}^+$

Table S9. IC_{50} values, photocytotoxicity indices (PI, IC_{50} dark/ IC_{50} irrad) and selection indices (SI, IC_{50} SV-HUC-1/ IC_{50} bladder cancer) for complexes **1** and **2** in SW-780 and VM-CUB-1 bladder cancer cells and SV-HUC-1 normal bladder epithelial cells after 1 h incubation, 1 h irradiation (blue 465nm, green 520 nm) and 72 h further incubation under normoxia (21% O_2) and hypoxia (1% O_2). CDDP (cisplatin) and complex **FM190** were studied for comparison.

Cell			**IC_{50} (μM)**[a]							
			Normoxia (21% O_2)				Hypoxia (1% O_2)			
			1	**2**	**FM190**	**CDDP**	**1**	**2**	**FM190**	**CDDP**
SW-780	Dark		15.1±3.9	>100	>50	2.5±0.4	14.4±0.3	>100	82.2±4.8	12.1±3.0
	465 nm[b]		1.6±0.3	4.4±2.8	7.4±0.9	3.1±0.1	1.1±0.3	2.4±1.3	13.3±2.6	14.2±4.5
	520 nm		13.4±3.5	69.1±14.3	46.3±5.5	3.0±0.3	1.7±1.0	4.5±2.6	60.5±0.5	13.5±7.9
	PI	Blue	9.4	>22.7	>6.7	-	13.1	>41.6	6.2	-
		Green	1.1	>1.4	>1.07	-	8.5	>22.2	1.4	-
	SI	Blue	7.6	3.3	2.0	0.6				
		Green	1.0	>1.4	>2.1	0.5				
VM-CUB-1	Dark		19.2±7.7	>100	>50	9.1±1.5	8.6±0.9	>100	59.4±14.8	12.8±2.7
	465 nm		3.2±0.6	2.5±0.1	6.7±2. 8	8.1±1.3	3.1±1.4	3.7±1.3	11.4±2.7	11.5±3.9
	520 nm		12.6±7.2	77.9±9.3	>50	8.3±3.1	1.2±0.1	4.25±0.03	34.5±0.5	15.5±0.2
	PI	Blue	6.0	>40.0	>7.46	-	2.8	>27.0	>5.2	-
		Green	1.5	>1.3	-	-	7.2	>23.5	>1.7	-
	SI	Blue	3.8	5.8	2.2	0.2				
		Green	1.0	>1.2	-	0.2				
SV-HUC-1	Dark		10.9±2.5	>100	>100	1.7±0.4				
	465 nm		12.1±3.8	14.4±3.3	14.6±6.0	1.97±0.02				
	520 nm		13.2±5.0	>100	>100	1.40±0.07				
	PI	Blue	-	>6.9	>6.8	-				
		Green	-	-	-	-				

[a] Each value is mean of at least two independent experiments; [b] Overly steep hill slope is observed in dose−response curves for cells treated with irradiation, which leads to poor fitting. The standard errors are based on the values from independent experiments, rather than from fitting curves.

Table S10. IC_{50} values and photocytotoxicity indices (PI) for complexes **3**−**6** in SW-780 bladder cancer cells after 1 h incubation, 1 h irradiation (blue 465nm, green 520 nm) and 72 h further incubation under normoxia (21% O_2) and hypoxia (1% O_2).

		IC_{50} (μM)[a]							
		Normoxia (21% O_2)				Hypoxia (1% O_2)			
		3	**4**	**5**	**6**	**3**	**4**	**5**	**6**
Dark		>100	>100	>100	74.4±0.9	>100	>100	>100	36.6±7.1
465 nm[b]		>100	9.3±2.7	8.4±2.0	7.0±2.0	>100	19.1±4.7	18.1±3.3	1.3±0.4
520 nm		>100	>100	58.1±2.8	46.2±2.8	>100	>100	>100	8.2±0.4
PI	Blue	-	>10.7	>11.9	10.6	-	>5.2	>5.5	28.2
	Green	-	-	>1.7	1.6	-	-	-	4.5

[a] Each value is mean of at least two independent experiments. [b] Overly steep hill slope is

observed in dose−response curves for cells treated with irradiation, which leads to poor fitting. The standard errors are based on the values from independent experiments, rather than from fitting curves.

Table S11. IC_{50} values and photocytotoxicity indices (PI) for complexes **1** and **2** in A2780 and A2780cis ovarian cancer cells and MRC-5 lung fibroblast cells after 1 h incubation, 1 h irradiation (blue 465nm, green 520 nm) and 72 h further incubation under normoxia (21% O_2) and hypoxia (1% O_2). CDDP (cisplatin) and complex **FM190** were studied for comparison.

Cell		**IC_{50} (μM)**[a]							
		Normoxia (21% O_2)				Hypoxia (1% O_2)			
		1	**2**	**FM190**[6]	**CDDP**[6]	**1**	**2**	**FM190**[6]	**CDDP**[6]
A2780	Dark	3.4±0.6	>100	11.6±1.8	0.7±0.1	9.9±1.8	>100	>100	7.6±0.5
	465 nm	1.0±0.3	2.9±0.9	1.1±0.1	0.9±0.5	0.7±0.2	1.7±0.6	1.0±0.2	8.8±1.7
	520 nm	3.2±0.7	27.9±4.2	9.9±1.6	0.82±0.03	0.7±0.2	33.0±18.0	18.0±6.3	9.6±2.3
	PI Blue	3.4	>34.5	10.5	-	14.1	>58.8	>100	-
	Green	1.1	>3.6	1.2	-	14.1	>3.0	>5.5	-
A2780cis	Dark	7.7±0.6	>100	21.7±0.1	9.7±1.4	14.8±0.3	>100	>100	14.9±3.2
	465 nm	3.6±0.4	0.84±0.06	2.8±0.7	7.67±0.04	0.59±0.08	1.7±0.3	1.4±0.3	16.2±1.0
	520 nm	7.5±1.3	20.0±7.3	19.3±1.8	10.2±1.2	0.9±0.3	3.8±1.7	12.2±1.3	16.5±2.9
	PI Blue	2.14	>119.0	7.8	-	25.1	>58.8	>71.4	-
	Green	1.03	>5.0	1.1	-	16.4	>26.3	>8.1	-
MRC-5	Dark	12.2±3.4	> 100	51.9±7.4	1.5±0.6				
	465 nm	2.6±0.9	8.9±4.7	9.8±1.5	1.5±0.3				
	520 nm	7.0±2.8	20.5±1.6	39.1±9.0	1.4±0.4				
	PI Blue	4.7	>11.2		-				
	Green	1.7	>4.87	1.3	-				

[a] Each value is mean of at least two independent experiments.

Table S12. Cyclic voltammogram data for complexes and corresponding ligands.

Compound	Pt^{IV}/Pt^{II}	$Ar\text{-}NO_2/Ar\text{-}NO_2^{\cdot -}$	
	E_{pc}	E_{pa}	E_{pc}
1	-0.974 V	-1.28 V	-1.367 V
2	-1.208, -1.506 V	-1.308 V	-1.376 V
FM190	-1.38 V	-	-
L1	-	-1.29 V	-1.38 V
L2	-	-1.454 V	-1.547 V

[a]E_{pa} and E_{pc} are the anodic and the cathodic peak potentials, respectively. Scan rate = 100 mV s^{-1}.

Table S13. Cellular accumulation of Pt (ng/10^6 cells) in cancer cells after exposure to complex **2** (10 μM).

Cell line	Conditions	Platinum accumulation (ng/10^6 cells)		
		Dark (2 h)	Irrad[a]	PI
A2780	Normoxia	1.1±0.2*	3.3±0.3***	3.0
A2780cis		0.69±0.03**	3.8±0.5**	5.5
SW-780		0.47±0.12*	2.6±0.3**	5.5
	Hypoxia	0.39±0.06**	62.0±14.1*	159.0

[a] 1 h incubation, 1 h irradiation (465 nm). All data were determined from triplicate samples and their statistical significance evaluated by a two-tail t-test with unequal variances. $^{*}p < 0.05$, $^{**}p < 0.01$, $^{***}p < 0.005$.

Table S14. Cellular distribution of Pt (%) in SW780 cells after exposure to complex **2** (10 μM).

Conditions	Platinum ratio (%)		
	Nuclei	Mitochondria	Cytoplasm
Normoxia	51.4±4.1	11.6±0.9	37.0±3.2
Hypoxia	67.2±9.5	8.3±0.5	24.5±8.9

Table S15. Accumulation of Pt (ng/mg) in rat bladder after exposure to complex **2** (50 μM).

Platinum accumulation (ng/mg)		
Dark (2 h)	Irrad[a]	PI
6.2±1.0	9.5±1.4*	1.5

[a] 1 h incubation, 1 h irradiation (465 nm). All data were determined from triplicate samples and their statistical significance evaluated by a two-tail t-test. *$p < 0.05$.

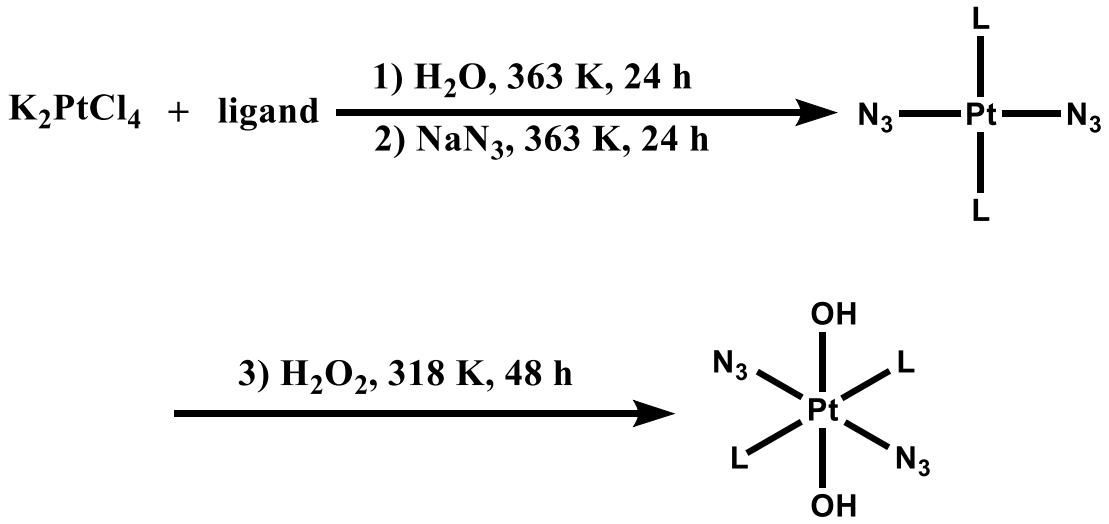

Scheme S1. The synthetic route for Pt(IV) complexes studied in this work.

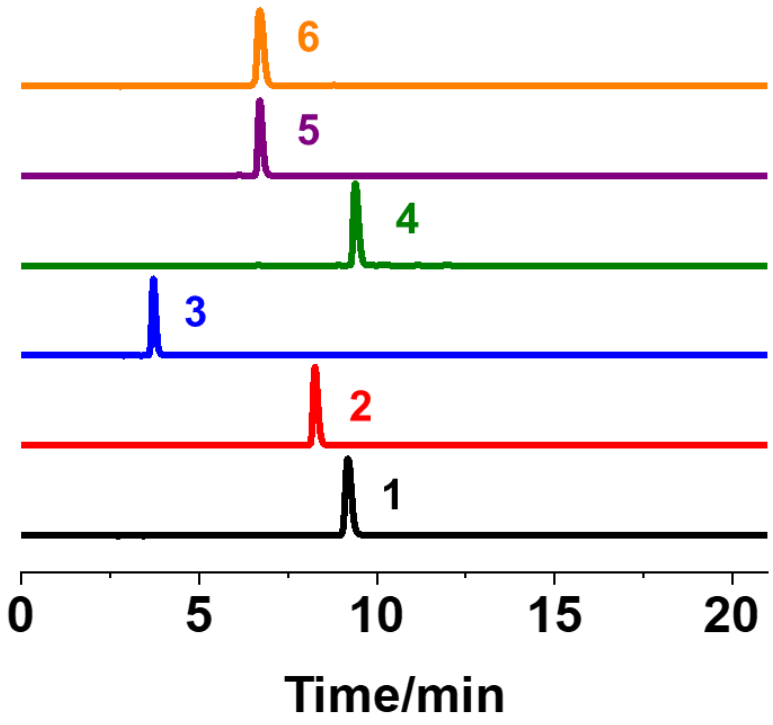

Figure S1. HPLC chromatograms for complexes **1**−**6** (detection wavelength at 254 nm, Mobile phase A: H_2O+0.1% TFA; B: ACN+0.1% TFA, 10-30% B in 10 min, 30% B for 5 min, 30-10% in 1 min, 10% for 5 min).

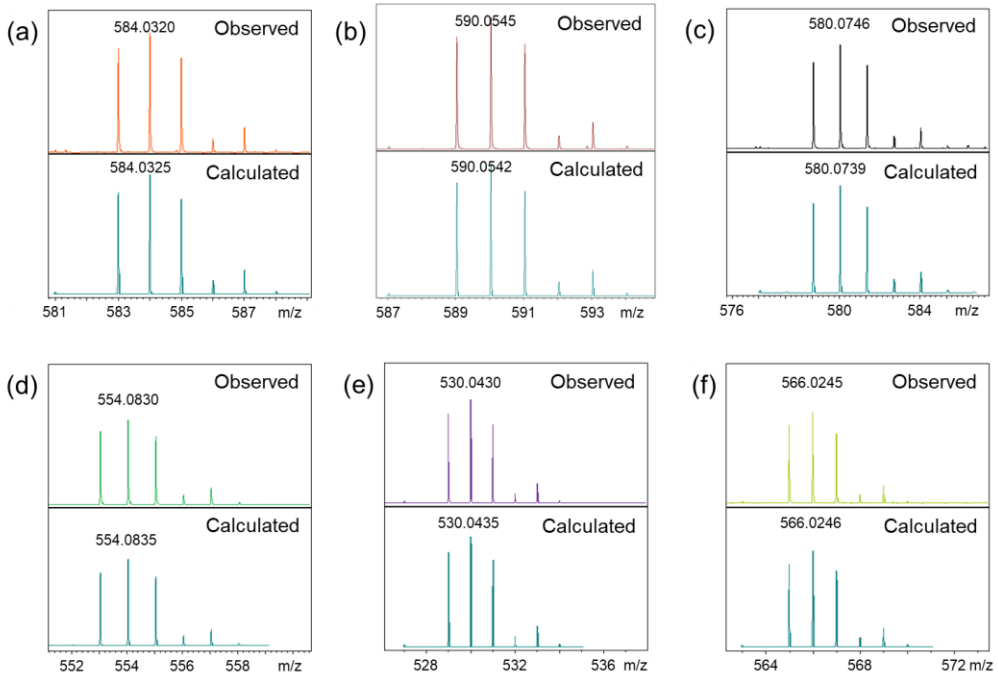

Figure S2. HR-ESI-MS for complexes (a) **1**, (b) **2**, (c) **3**, (d) **4**, (e) **5**, and (f) **6**.

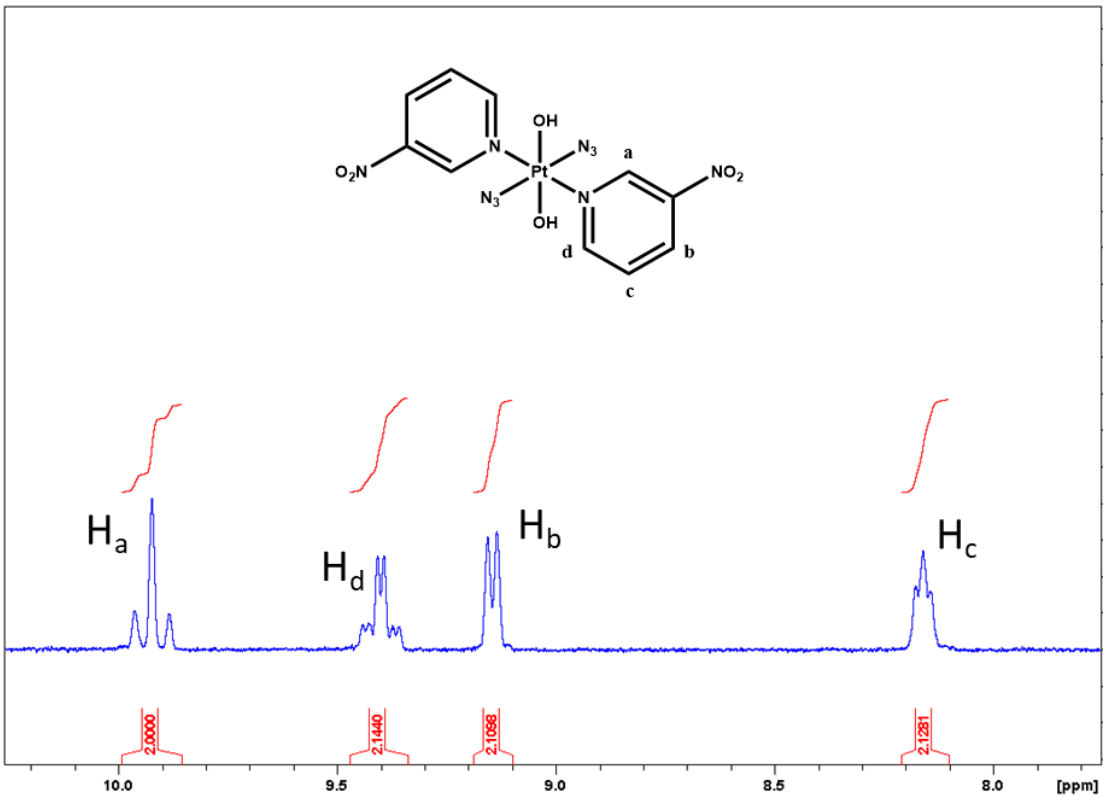

Figure S3. 400 Hz ^{1}H NMR spectrum of complex **1** in MeOD-*d*$_4$ at 298 K.

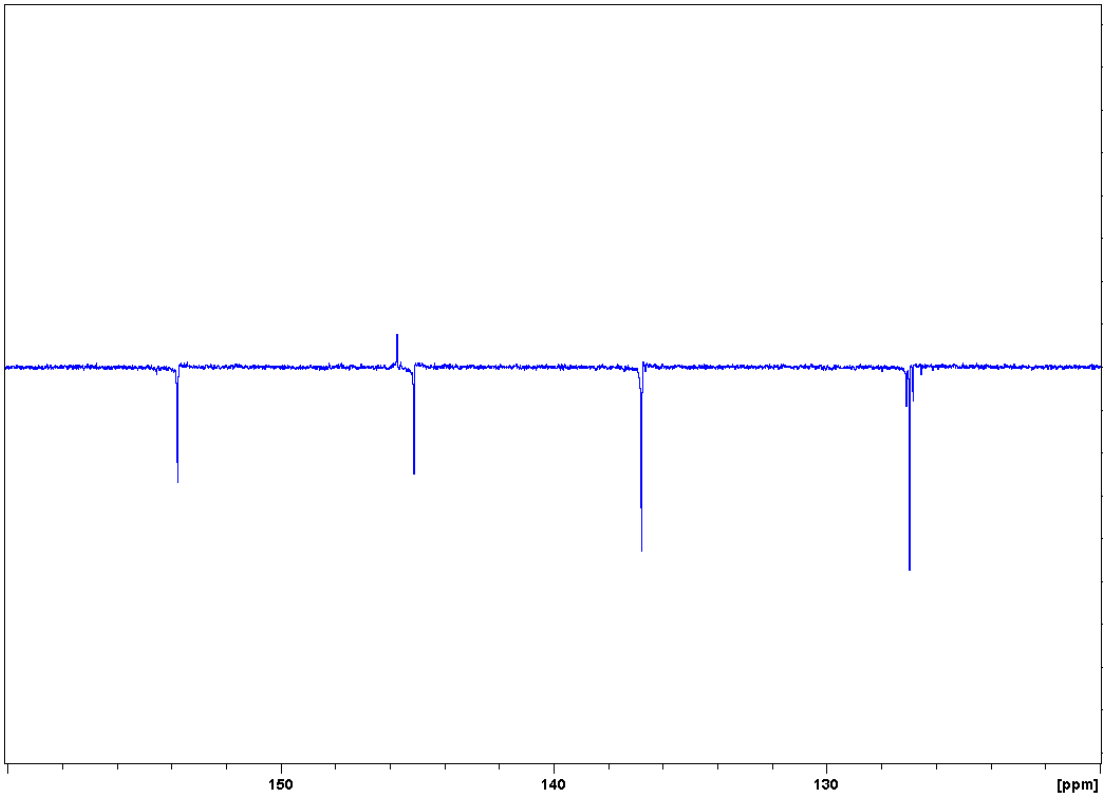

Figure S4. 125 Hz ^{13}C-{^{1}H} APT NMR spectrum of complex **1** in MeOD-*d*$_4$ at 298 K.

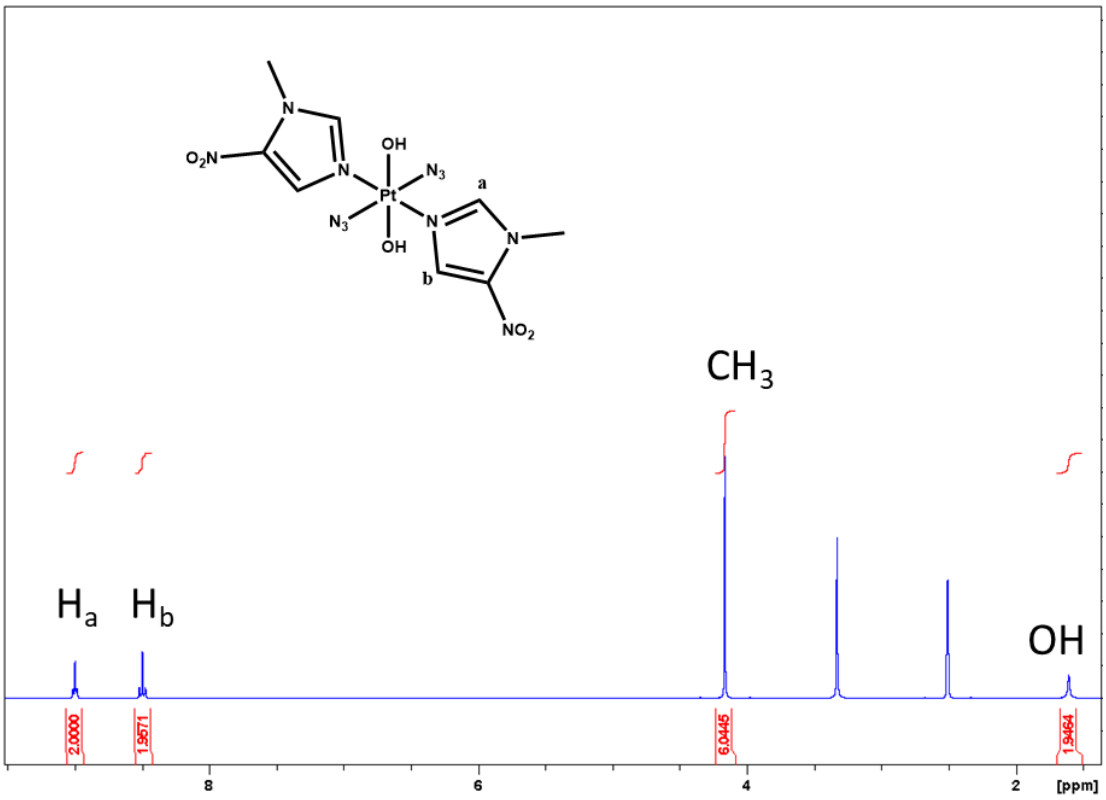

Figure S5. 400 Hz ^{1}H NMR spectrum of complex **2** in DMSO-d_6 at 298 K.

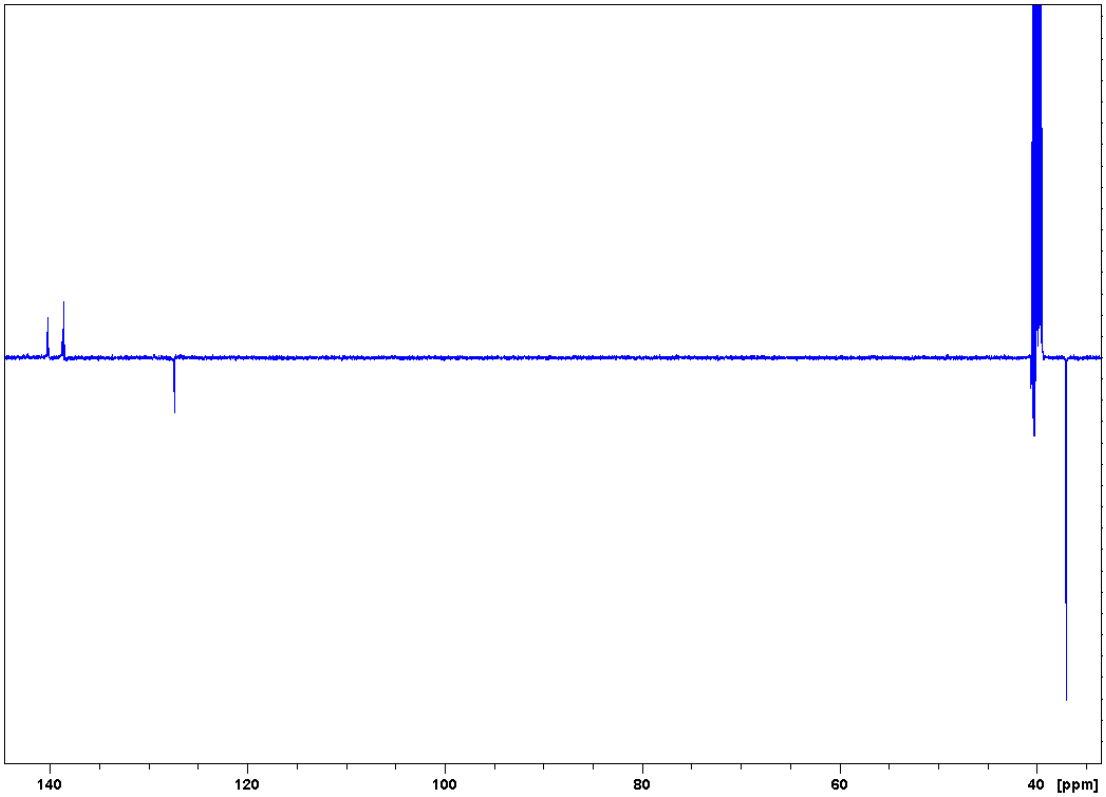

Figure S6. 125 Hz ^{13}C-{^{1}H} APT NMR spectrum of complex **2** in DMSO-d_6 at 298 K.

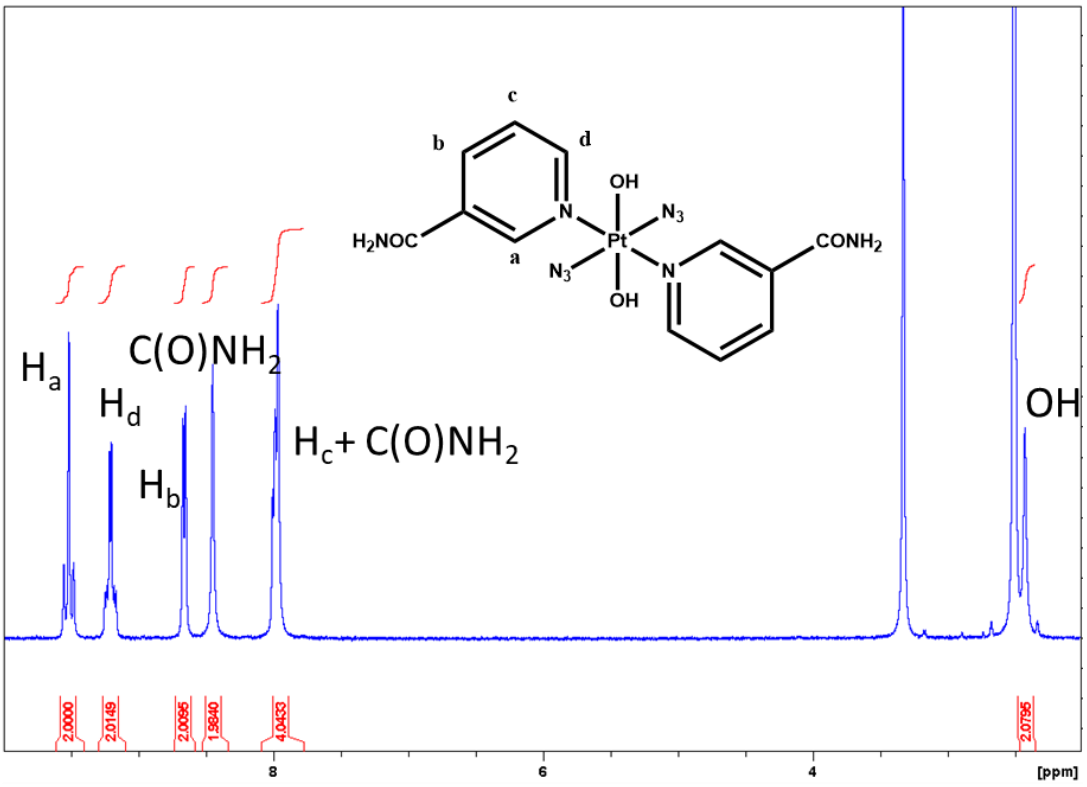

Figure S7. 500 Hz ^{1}H NMR spectrum of complex **3** in DMSO-d_6 at 298 K.

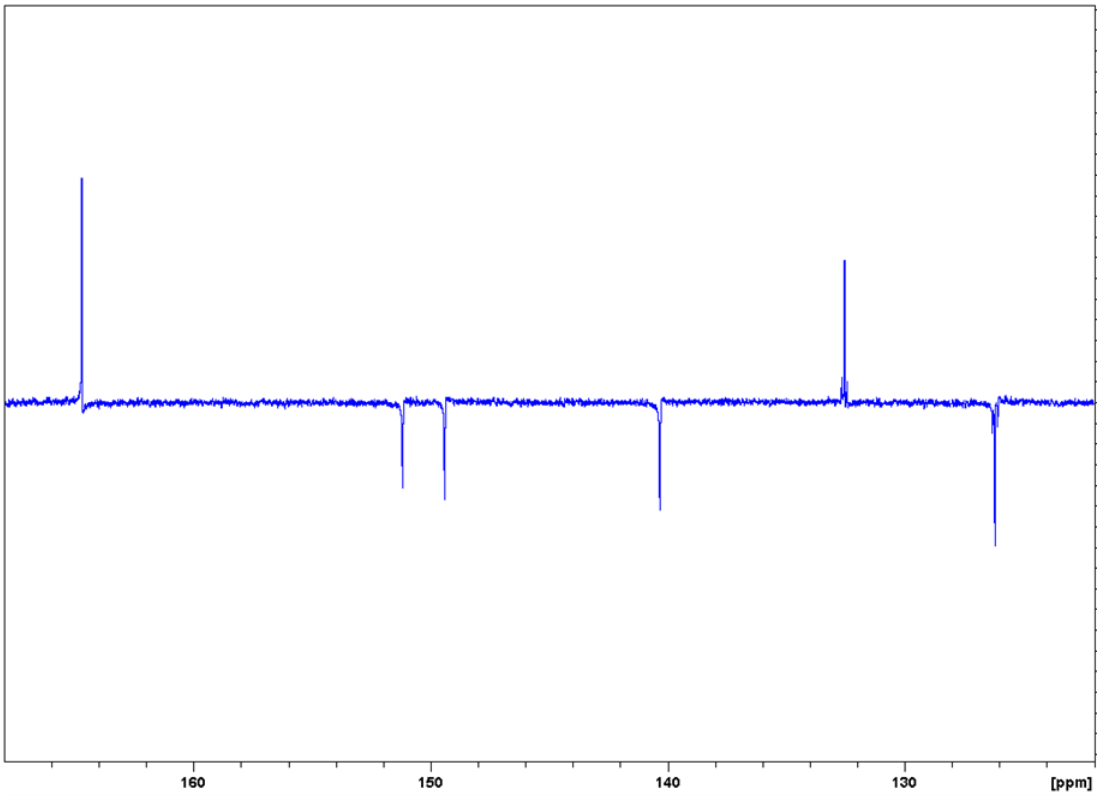

Figure S8. 125 Hz ^{13}C-{^{1}H} APT NMR spectrum of complex **3** in DMSO-d_6 at 298 K.

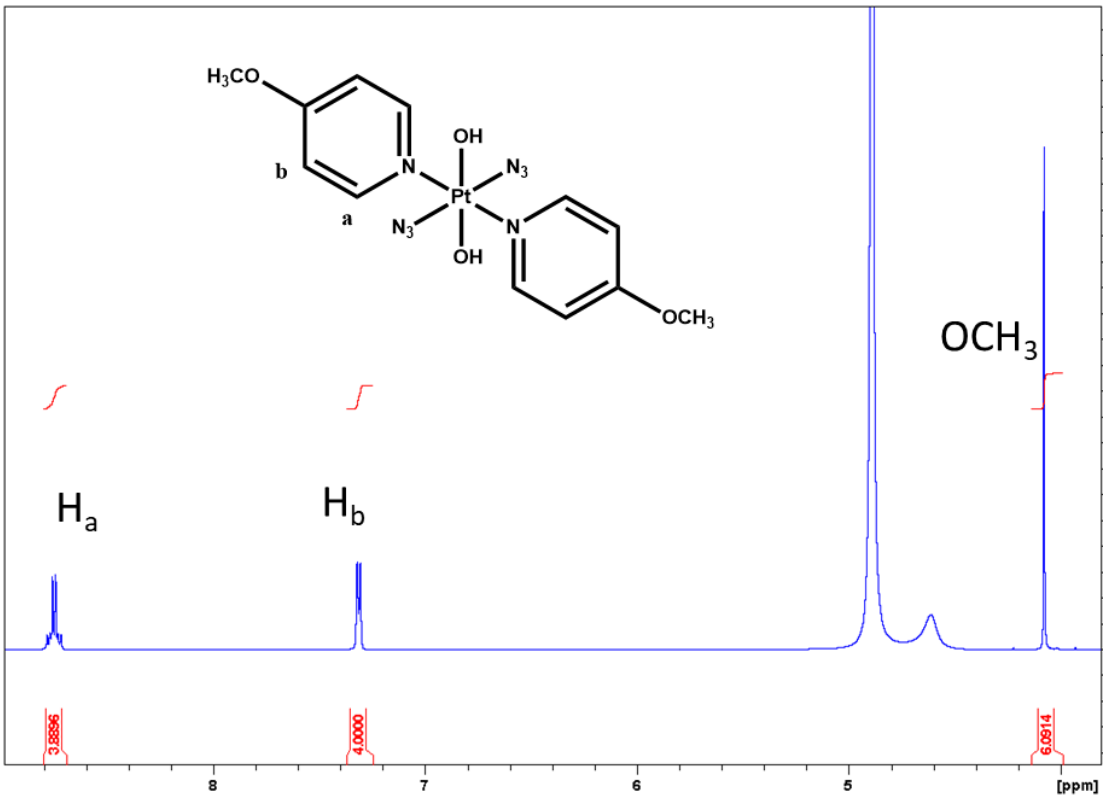

Figure S9. 500 Hz ^{1}H NMR spectrum of complex **4** in MeOD-*d*$_4$ at 298 K.

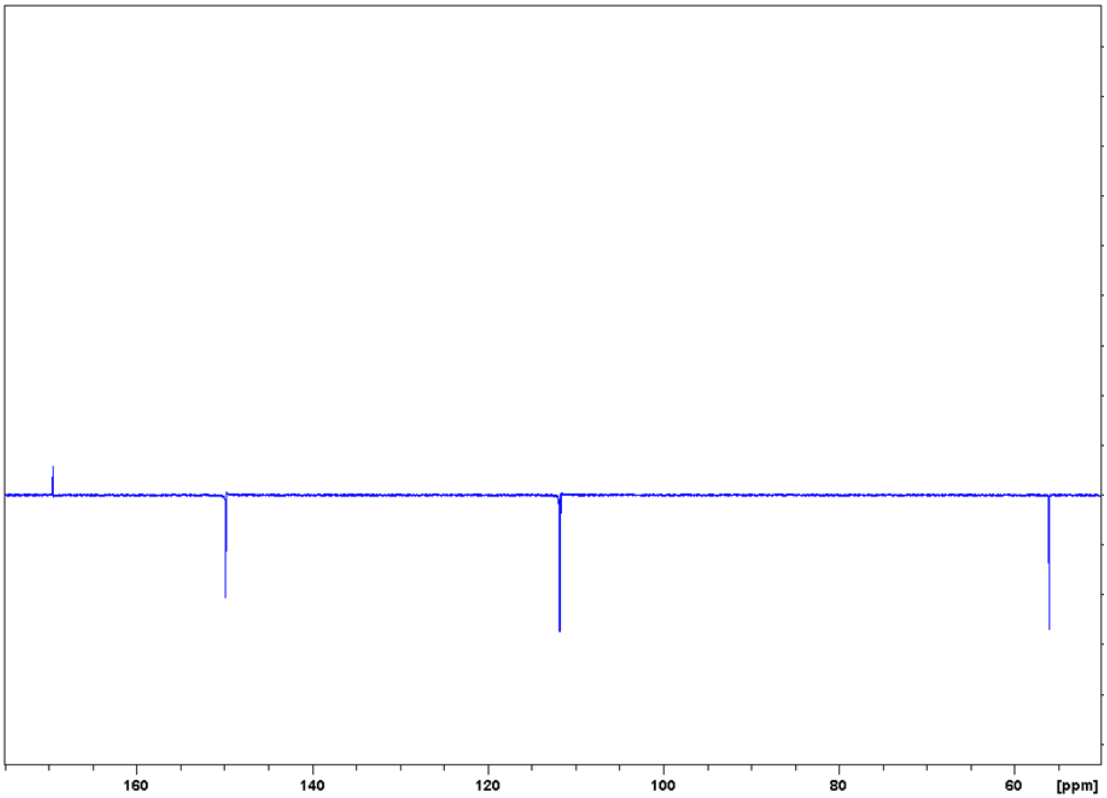

Figure S10. 125 Hz ^{13}C-{^{1}H} APT NMR spectrum of complex **4** in MeOD-*d*$_4$ at 298 K.

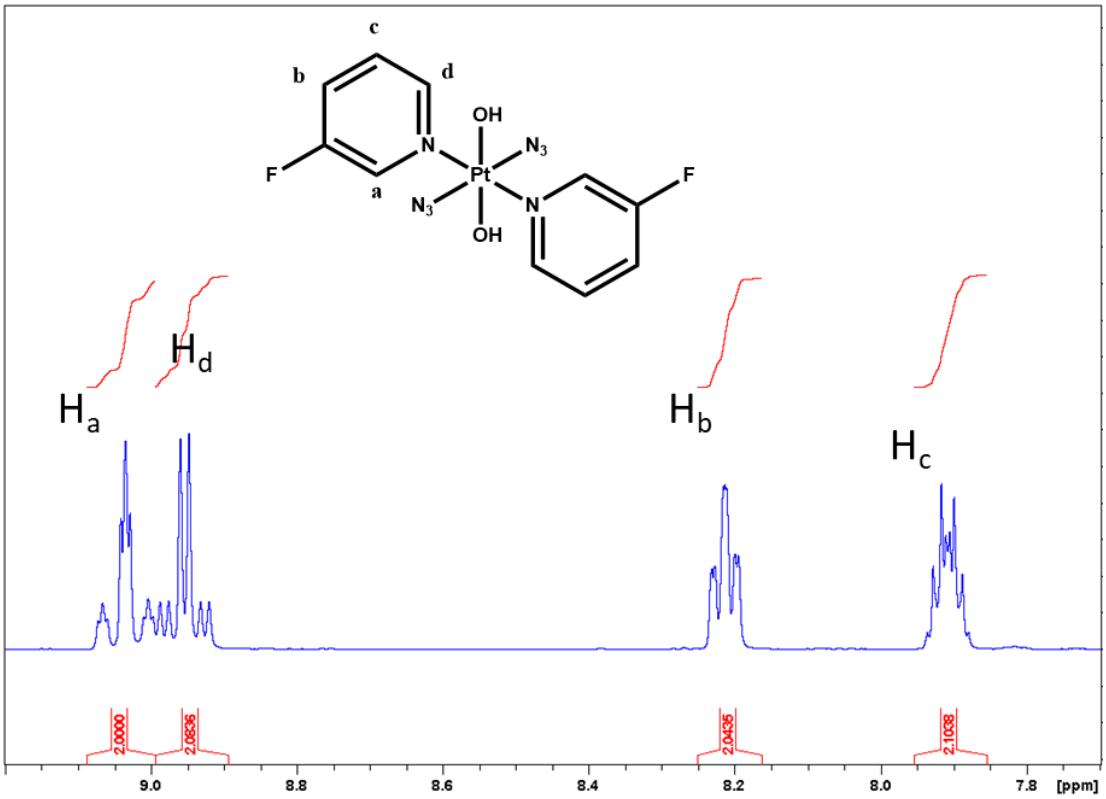

Figure S11. 500 Hz ^{1}H NMR spectrum of complex **5** in MeOD-*d*$_4$ at 298 K.

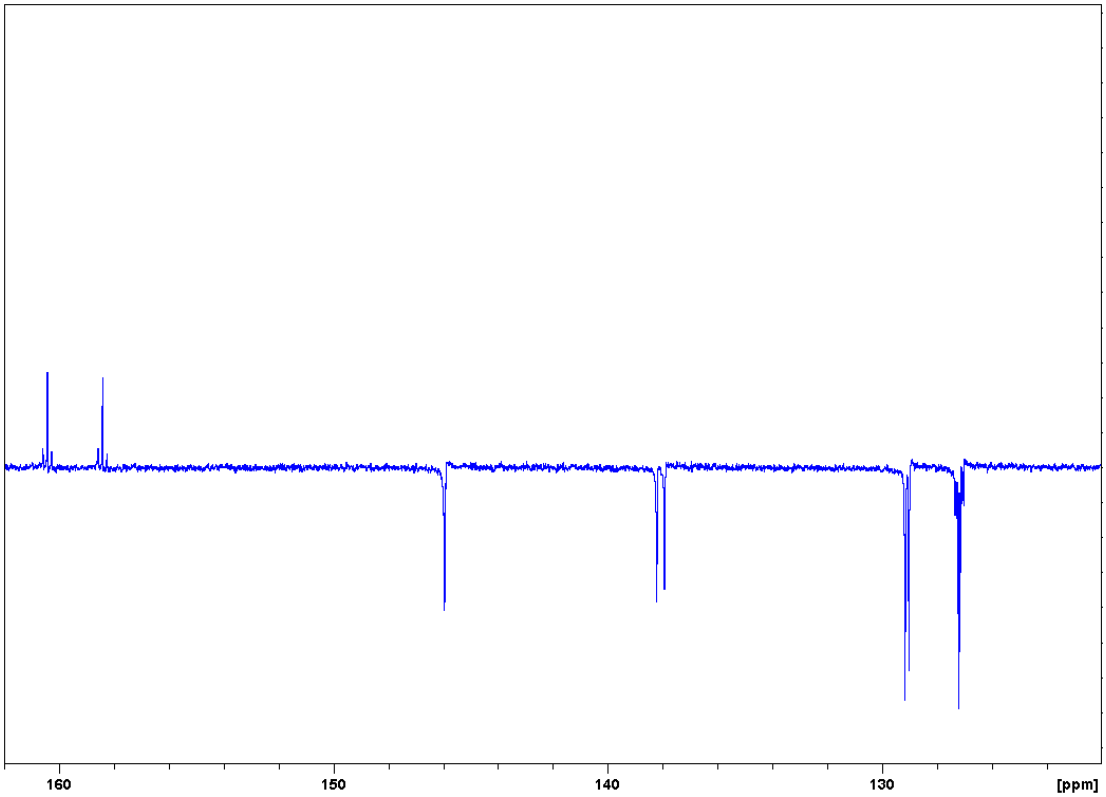

Figure S12. 125 Hz ^{13}C-{^{1}H} APT NMR spectrum of complex **5** in MeOD-*d*$_4$ at 298 K.

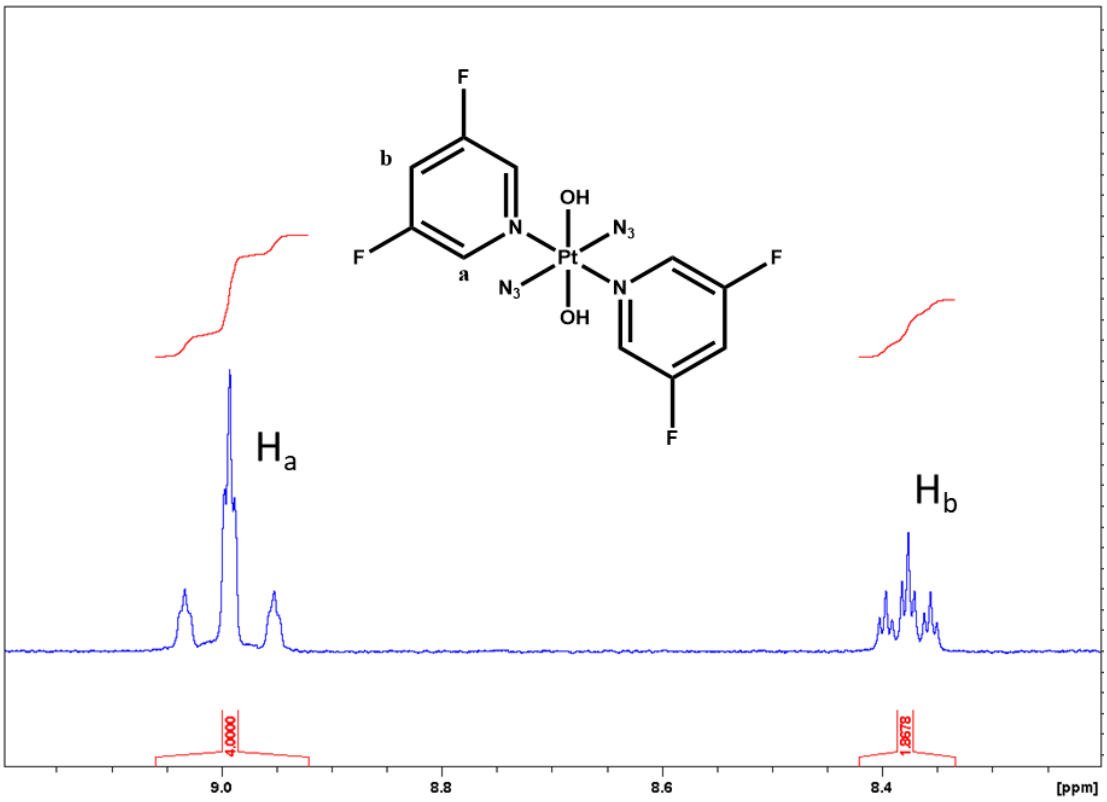

Figure S13. 400 Hz ^{1}H NMR spectrum of complex **6** in MeOD-*d*$_4$ at 298 K.

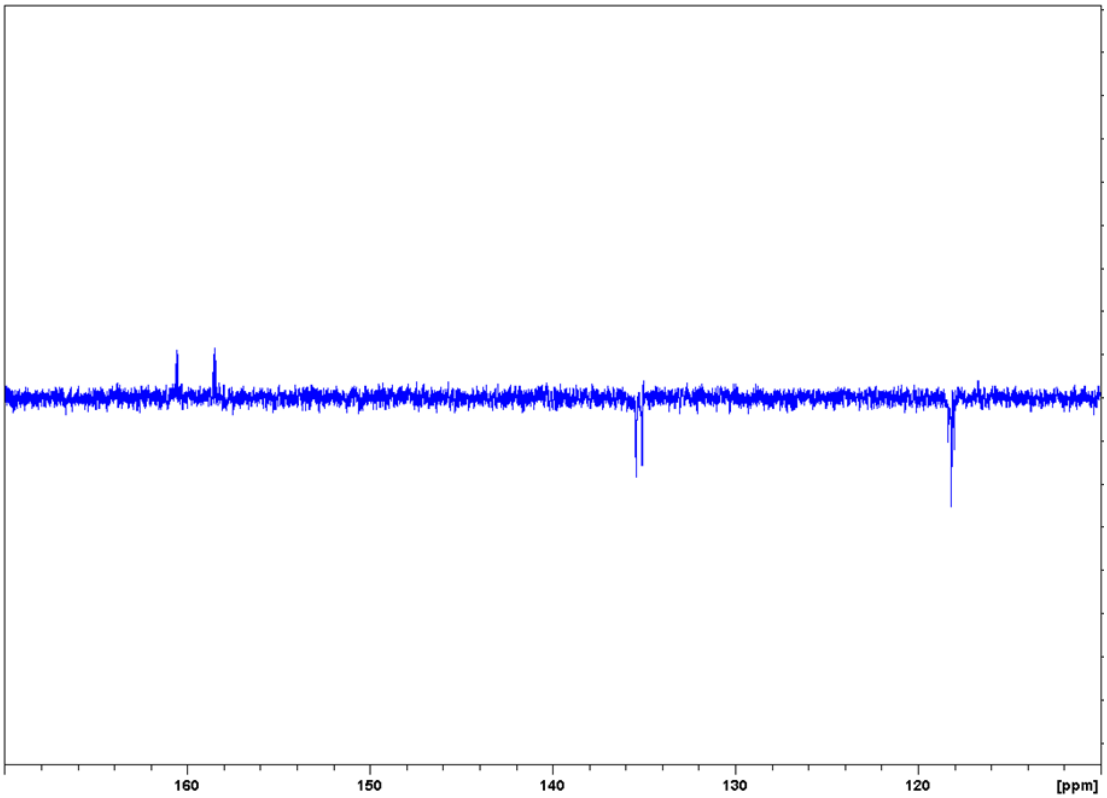

Figure S14. 125 Hz ^{13}C-{^{1}H} APT NMR spectrum of complex **6** in MeOD-*d*$_4$ at 298 K.

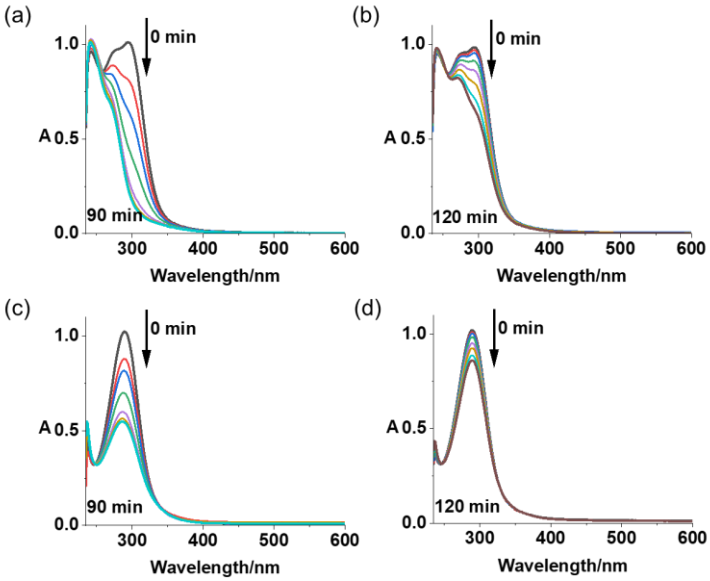

Figure S15. UV-vis spectral changes for complexes **1** and **2** in N_2-saturated H_2O exposed to blue (463 nm, a for **1**; c for **2**) or green (517 nm, b for **1**; d for **2**) light at 298 K, recorded at 0, 5, 10, 20, 40, 60, 90 and 120 min.

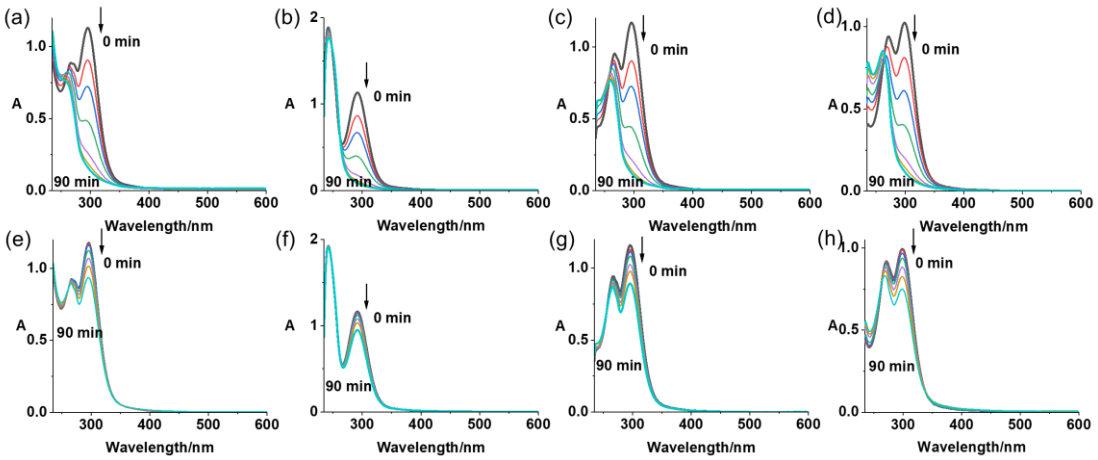

Figure S16. UV-vis spectral changes for complexes **3**–**6** in in air-saturated H_2O exposed to blue (463 nm, a for **3**; b for **4**; c for **5**; d for **6**) or green (517 nm, e for **3**; f for **4**; g for **5**; h for **6**) light at 298 K, recorded at 0, 5, 10, 20, 40, 60 and 90 min.

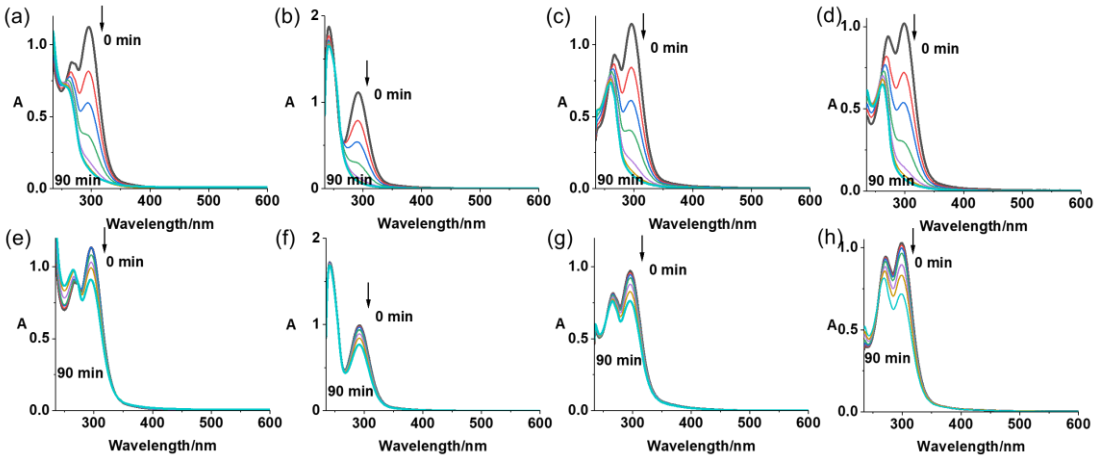

Figure S17. UV-vis spectral changes for complexes **3**–**6** in in N_2-saturated H_2O exposed to blue (463 nm, a for **3**; b for **4**; c for **5**; d for **6**) or green (517 nm, e for **3**; f for **4**; g for **5**; h for **6**) light at 298 K, recorded at 0, 5, 10, 20, 40, 60, 90 and 120 min.

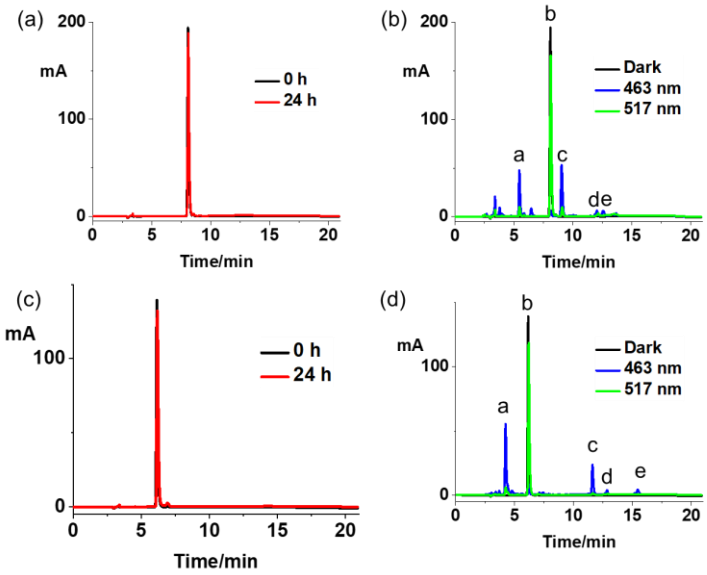

Figure S18. Dark stability for 24 h at 310 K (a for **1**; c for **2**) and photochemical decomposition upon 1 h irradiation with blue or green light (b for **1**; d for **2**) of 50 μM complexes determined by HPLC. Mobile phase A: H_2O+0.1% FA; B: ACN+0.1% FA, 10-30% B in 10 min, 30% B for 5 min, 30-10% in 1 min, 10% for 5 min). Possible photoproducts a–e are listed in Tables **S7** and **S8**.

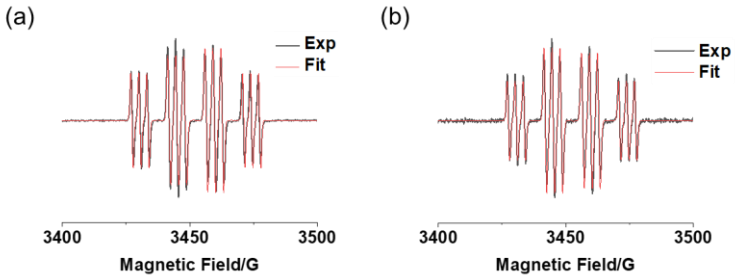

Figure S19. Observed (black) and simulated (red) EPR spectra of complex (2.5 mM) and DMPO (40 mM) in MilliQ water (containing 5% DMSO) showing the formation of DMPO−N_3• adducts after irradiation (463 nm). The experimental trace is the accumulation of 50 scans (conversion time 10.24 ms, time constant 10.24 ms, and sweep time 20.97 s for each scan) with continuous irradiation (463 nm). Parameters for simulation: (a) **1**: DMPO−N_3• (g = 2.00536, $\boldsymbol{a}_{\mathbf{NO}}^{\mathbf{N}}$ = 1.44 mT, $\boldsymbol{a}_{\boldsymbol{\beta}}^{\mathbf{H}}$ = 1.44 mT, and $\boldsymbol{a}_{\mathbf{N}\alpha}^{\mathbf{N}}$ = 0.30 mT); (b) **2**. Parameters for simulation: DMPO−N_3• (g = 2.00528, $\boldsymbol{a}_{\mathbf{NO}}^{\mathbf{N}}$ = 1.44 mT, $\boldsymbol{a}_{\boldsymbol{\beta}}^{\mathbf{H}}$ = 1.44 mT, and $\boldsymbol{a}_{\mathbf{N}\alpha}^{\mathbf{N}}$ = 0.30 mT).

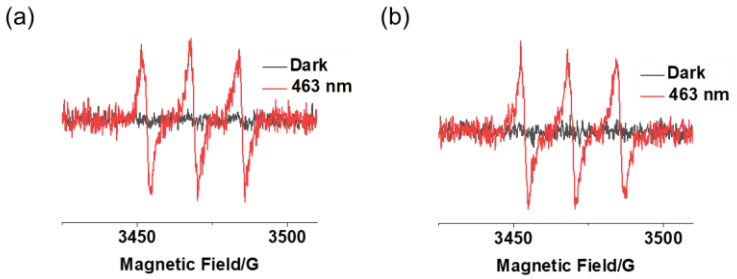

Figure S20. EPR spectra of complexes (2.5 mM) (a) **1** and (b) **2** in the presence of TEMP (20 mM) in acetonitrile (containing 5% DMSO) to trap singlet oxygen; Dark (—); blue light (—, 463 nm). The experimental trace is the accumulation of 5 scans (conversion time 10.24 ms, time constant 10.24 ms, and sweep time 20.97 s for each scan) after continuous irradiation (463 nm, 17.5 min). Parameters for simulation: (a) **1**: TEMPO (g = 2.00606, $\boldsymbol{a}_{\mathbf{NO}}^{\mathbf{N}}$ = 1.64 mT); (b) TEMPO (g = 2.00566, $\boldsymbol{a}_{\mathbf{NO}}^{\mathbf{N}}$ = 1.59 mT).

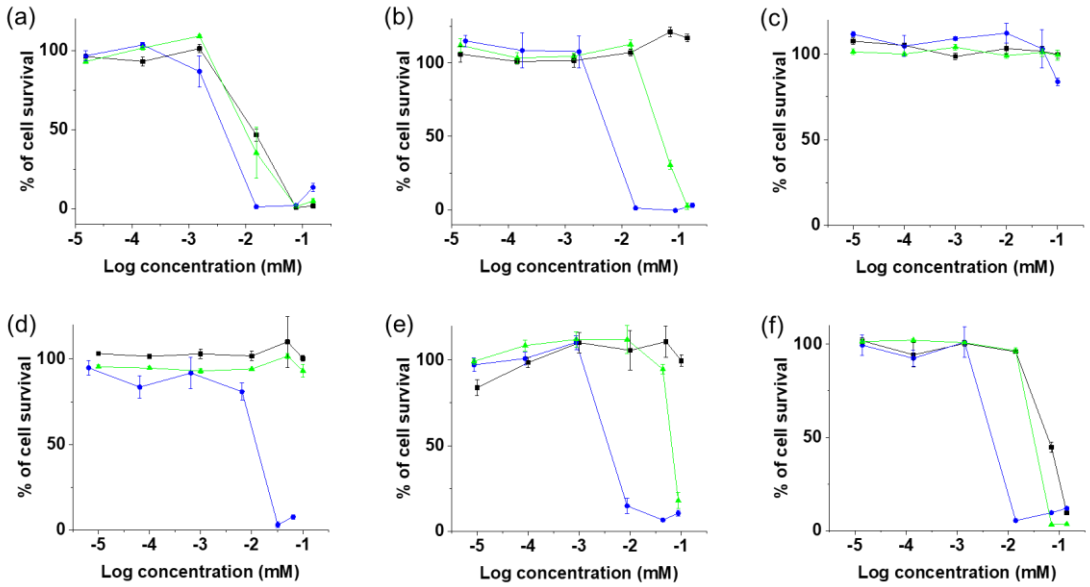

Figure S21. Growth inhibition curves for SW780 bladder cancer cells treated with complexes (a) **1**, (b) **2**, (c) **3**, (d) **4**, (e) **5**, and (f) **6** after 1 h incubation, 1 h irradiation (blue 465nm, green 520 nm) and 72 h further incubation under normoxia (21% O_2). ■ for dark; ● for blue light; ▲ for green light. Overly steep hill slope is observed in some dose−response curves for cells treated with irradiation, which leads to poor fitting. The standard errors are based on the values from independent experiments, rather than from fitting curves.

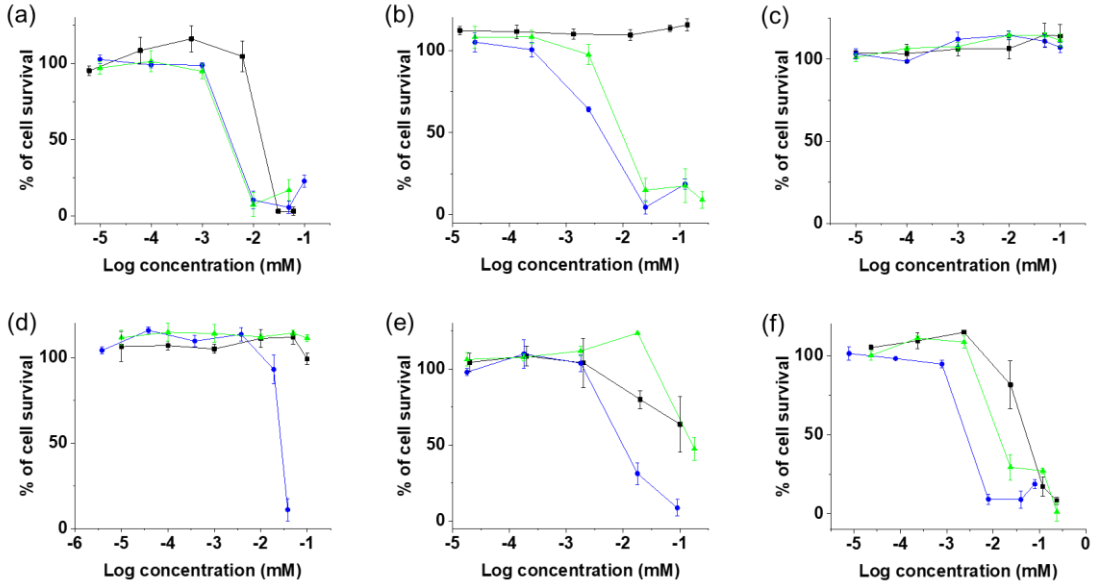

Figure S22. Growth inhibition curves for SW780 bladder cancer cells treated with complexes (a) **1**, (b) **2**, (c) **3**, (d) **4**, (e) **5**, and (f) **6** after 1 h incubation, 1 h irradiation (blue 465nm, green 520 nm) and 72 h further incubation under hypoxia (1% O_2). ■ for Dark; ● for blue light; ▲ for green light. Overly steep hill slope is observed in some dose−response curves for cells treated with irradiation, which leads to poor fitting. The standard errors are based on the values from independent experiments, rather than from fitting curves.

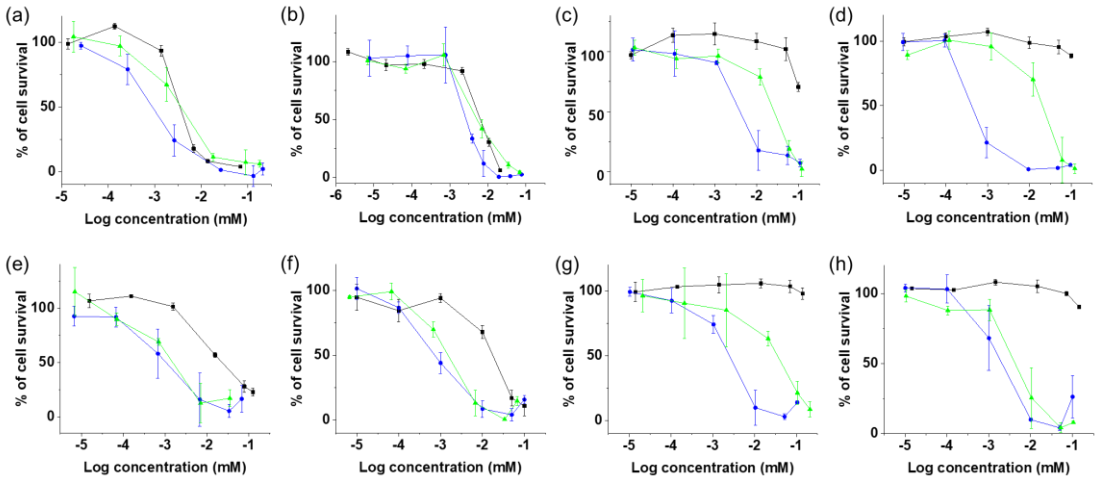

Figure S23. Growth inhibition curves for ovarian cancer cells treated with complexes after 1 h incubation, 1 h irradiation (blue 465nm, green 520 nm) and 72 h further incubation under normoxia (a, A2780, **1**; b, A2780cis, **1**; c, A2780, **2**; d, A2780cis, **2**) or hypoxia (e, A2780, **1**; f, A2780cis, **1**; g, A2780, **2**; h, A2780cis, **2**). ■ for Dark; ● for blue light; ▲ for green light. Overly steep hill slope is observed in some dose−response curves for cells treated with irradiation, which leads to poor fitting. The standard errors are based on the values from independent experiments, rather than from fitting curves.

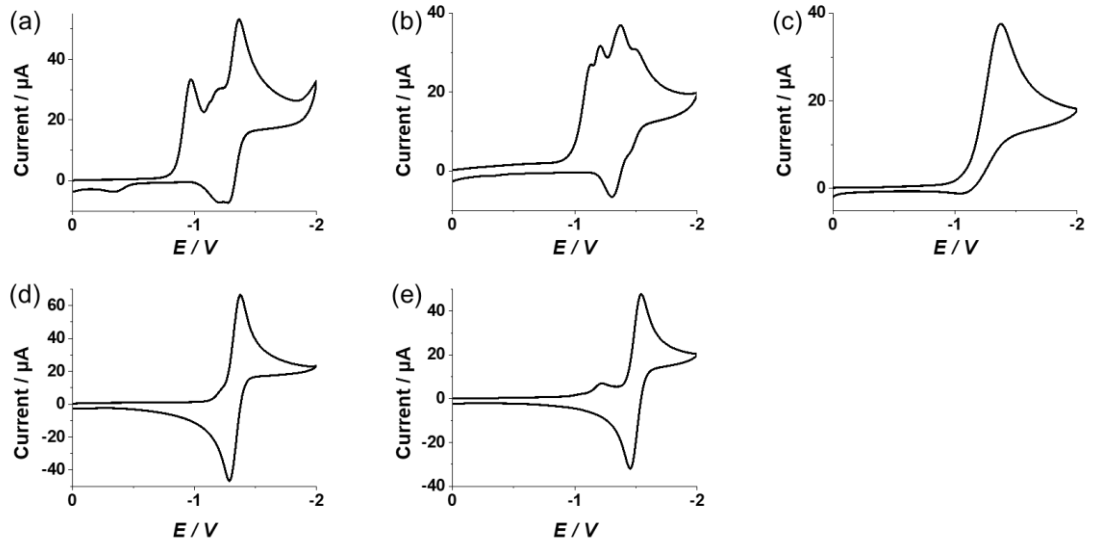

Figure S24. Cyclic voltammograms for complexes (a) **1**, (b) **2**, and (c) **FM190**, and ligands (d) **L1** and (e) **L2** (1 mM) in 0.1 M NBu_4PF_6-ACN (under N_2).

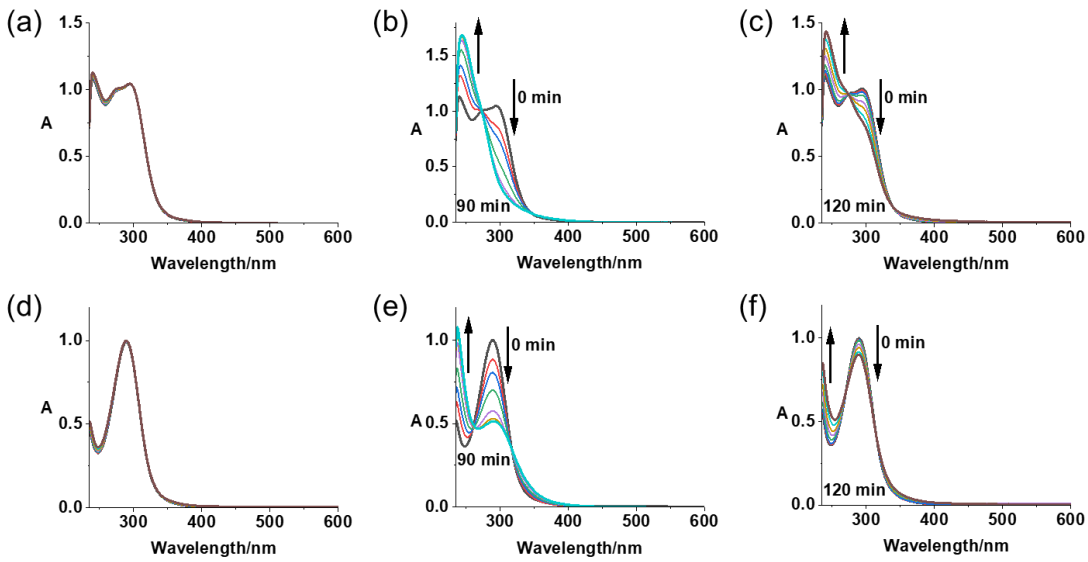

Figure S25. UV-vis spectral changes for complexes **1** and **2** in the presence of 2 mM GSH in air-saturated PBS in the dark (120 min, a for **1**; d for **2**) or exposed to blue (463 nm, b for **1**; e for **2**) or green (517 nm, c for **1**; f for **2**) light at 298 K.

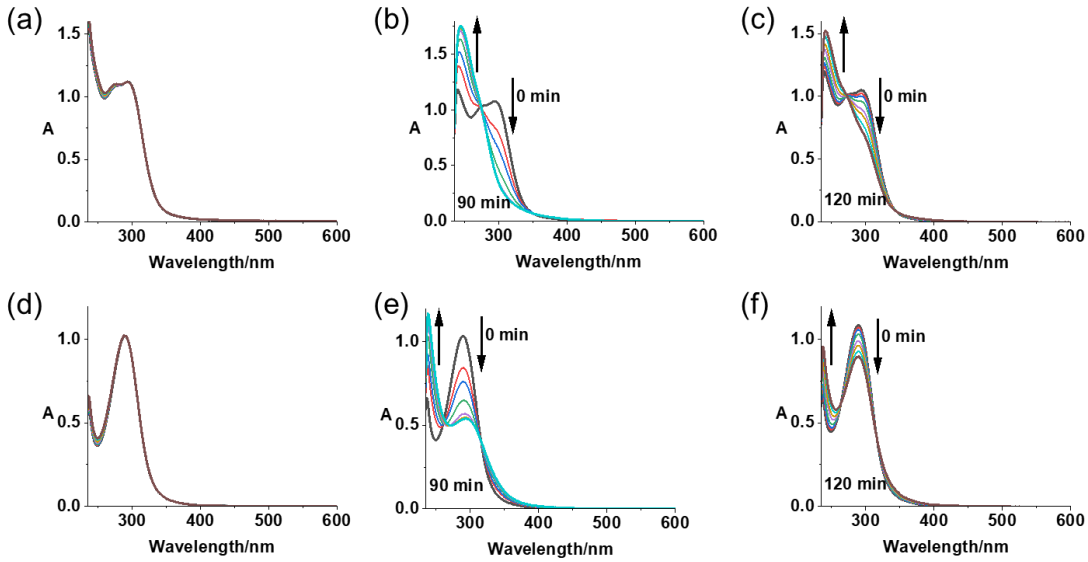

Figure S26. UV-vis spectral changes of complexes **1** and **2** in the presence of 2 mM GSH in N_2-saturated PBS in the dark (120 min, a for **1**; d for **2**) or exposed to blue (463 nm, b for **1**; e for **2**) or green (517 nm, c for **1**; f for **2**) light at 298 K.

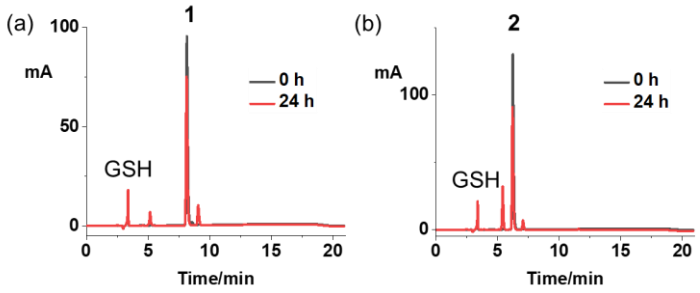

Figure S27. Dark stability for 24 h at 310 K (a for **1**; b for **2**) of 50 μM complexes in the presence of 2 mM GSH determined by HPLC. Mobile phase A: H_2O+0.1% FA; B: ACN+0.1% FA, 10−30% B in 10 min, 30% B for 5 min, 30−10% in 1 min, 10% for 5 min).

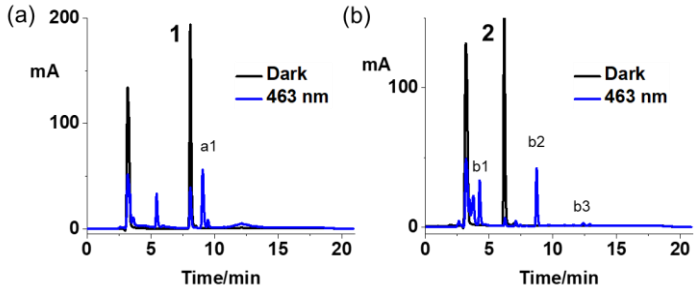

Figure S28. HPLC traces (detection at 254 wavelength) for the photoreactions between complexes (a. **1**, b. **2**) and 2 mol. equiv. of 5′-GMP after 1 h irradiation, dark (—) and blue light (—, 463 nm). Mobile phase A: H_2O+0.1% FA; B: ACN+0.1% FA, 10−30% B in 10 min, 30% B for 5 min, 30−10% in 1 min, 10% for 5 min).

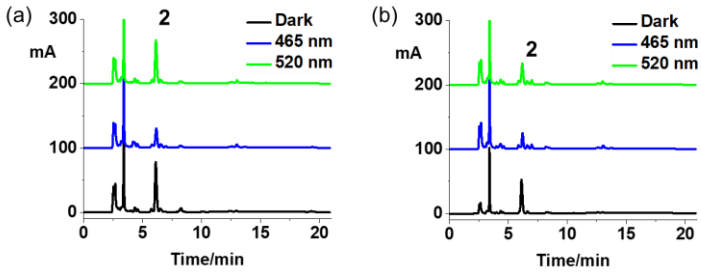

Figure S29. HPLC traces (detection at 254 wavelength) for the supernatant containing **2** and its photoproducts collected after incubation with SW780 cells, dark (—), blue (—, 463 nm) and green (—, 520 nm) light. Mobile phase A: H_2O+0.1% FA; B: ACN+0.1% FA, 10−30% B in 10 min, 30% B for 5 min, 30−10% in 1 min, 10% for 5 min).

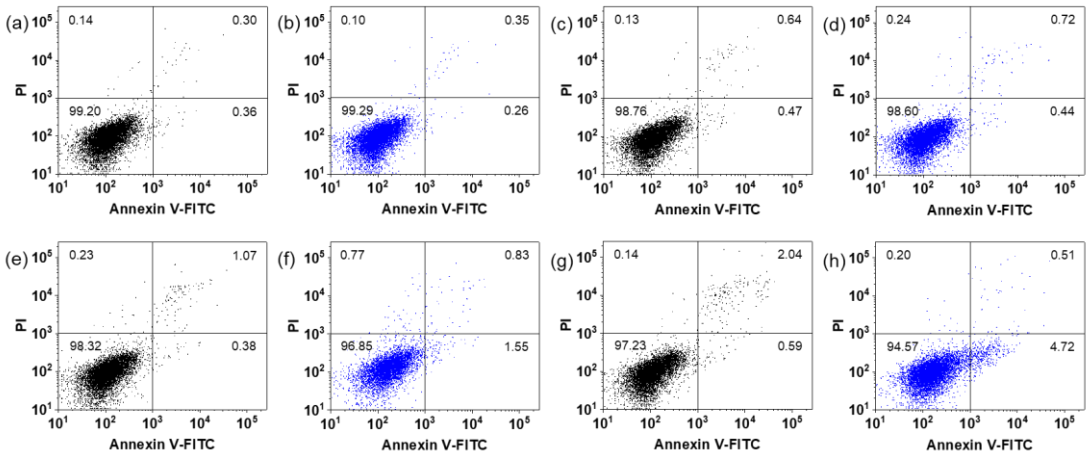

Figure S30. Cell apoptosis assay for SW780 cells under hypoxia double-stained by Annexin V-FITC/PI ($\lambda_{ex}/\lambda_{em}$ = 488/500–560 nm for Annexin V-FITC, $\lambda_{ex}/\lambda_{em}$ = 488/645–735 nm for PI) and analysed by flow cytometry. a) untreated SW780 cells in the dark; b) untreated SW780 cells irradiated with blue light (465 nm); c) SW780 cells treated with cisplatin (10 μM) in the dark and d) irradiated with blue light; e) SW780 cells treated with **2** (10 μM) in the dark and f) irradiated with blue light; g) SW780 cells treated with **2** (20 μM) in the dark and h) irradiated with blue light. Percentage of cells in each status are shown.

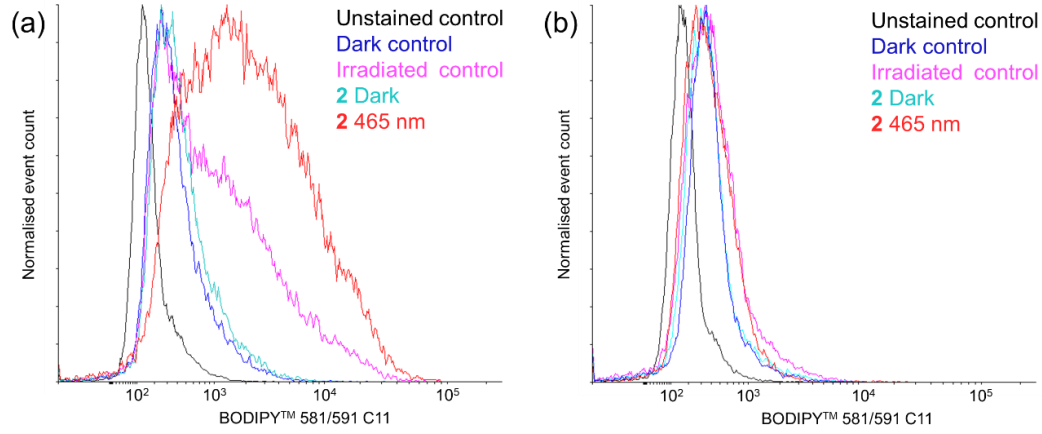

Figure S31. Lipid peroxidation assay for SW780 cells under (a) normoxia and (b) hypoxia stained by BODIPY™ 581/591 C11 ($\lambda_{ex}/\lambda_{em}$ = 488/500–560 nm) and analysed by flow cytometry. X-axis indicates the intensity of emission from oxidised BODIPY™ 581/591 C11.

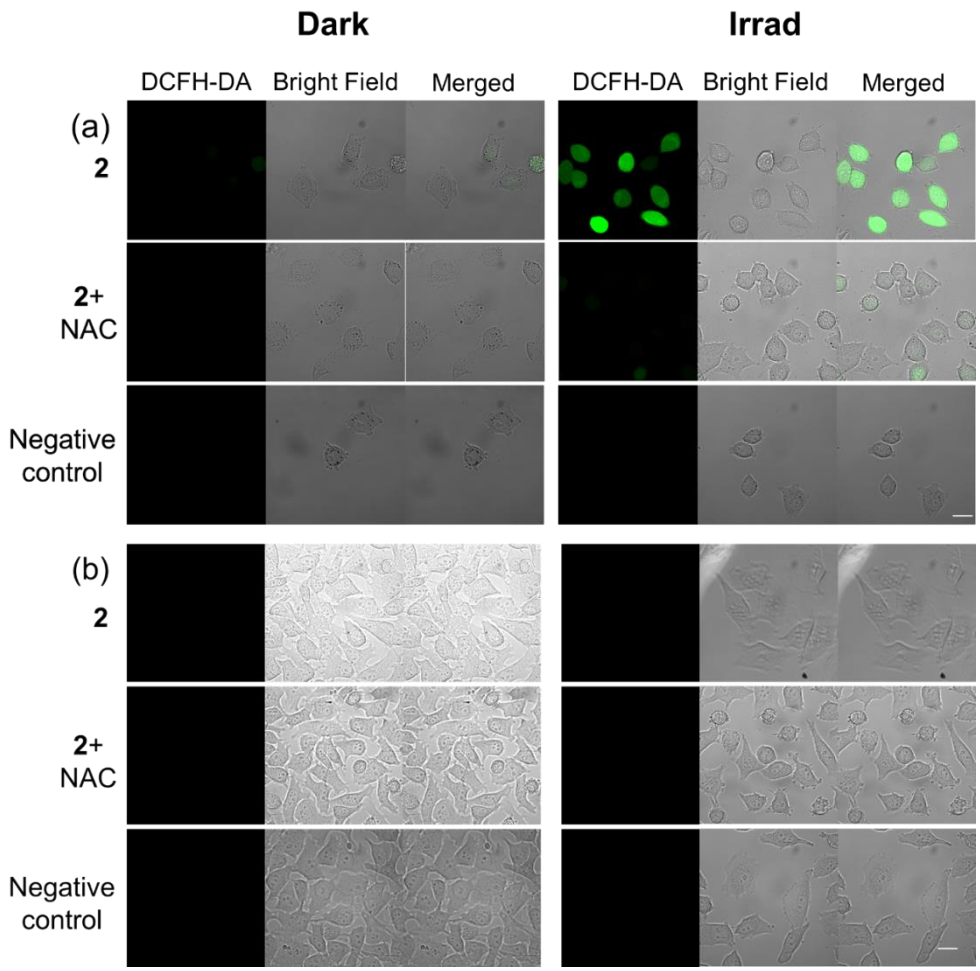

Figure S32. Confocal fluorescence microscopy images of ROS generation of SW780 cells treated with **2** (10 μM) in the dark or irradiated (465 nm) then probed by DCFH-DA (20 μM, λ_{ex} = 488 nm, λ_{em} = 501–627 nm) in the absence and presence of antioxidant *N*-acetyl-L-cysteine (NAC, 10 mM) under (a) normoxia and (b) hypoxia. SW780 cells without **2** were used as a negative control. Scale bar = 20 μm.

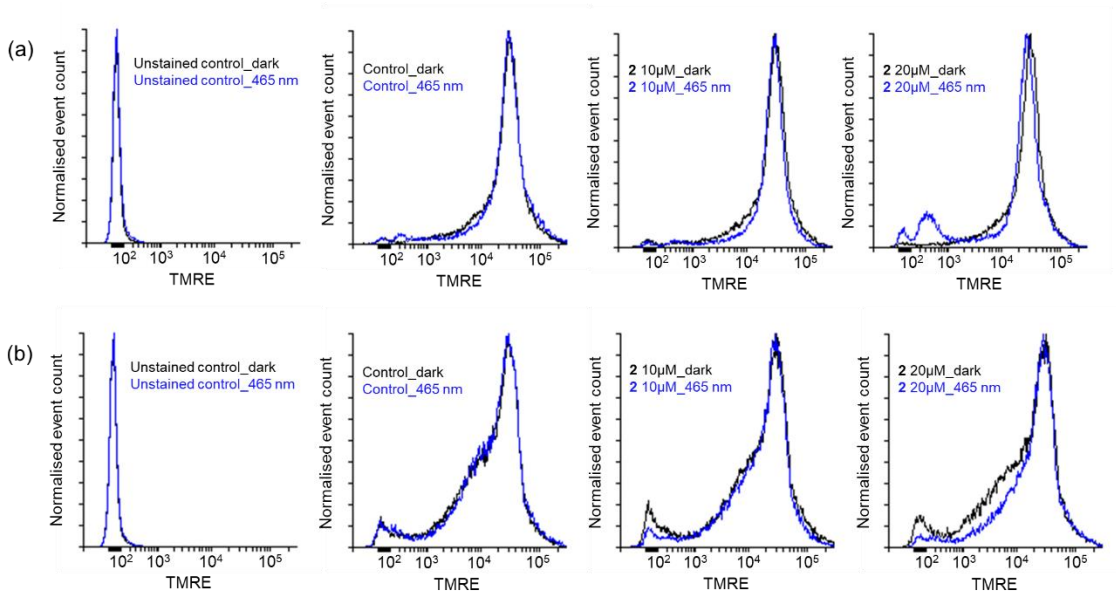

Figure S33. Mitochondrial potential of SW780 cells treated with **2** (0, 10 and 20 μM) in the dark (2 h) or 1 h incubation and 1 h irradiation (465 nm) under (a) normoxia or (b) hypoxia, then stained by TMRE ($\lambda_{ex}/\lambda_{em}$ = 561/570−600 nm) and analysed by flow cytometry.

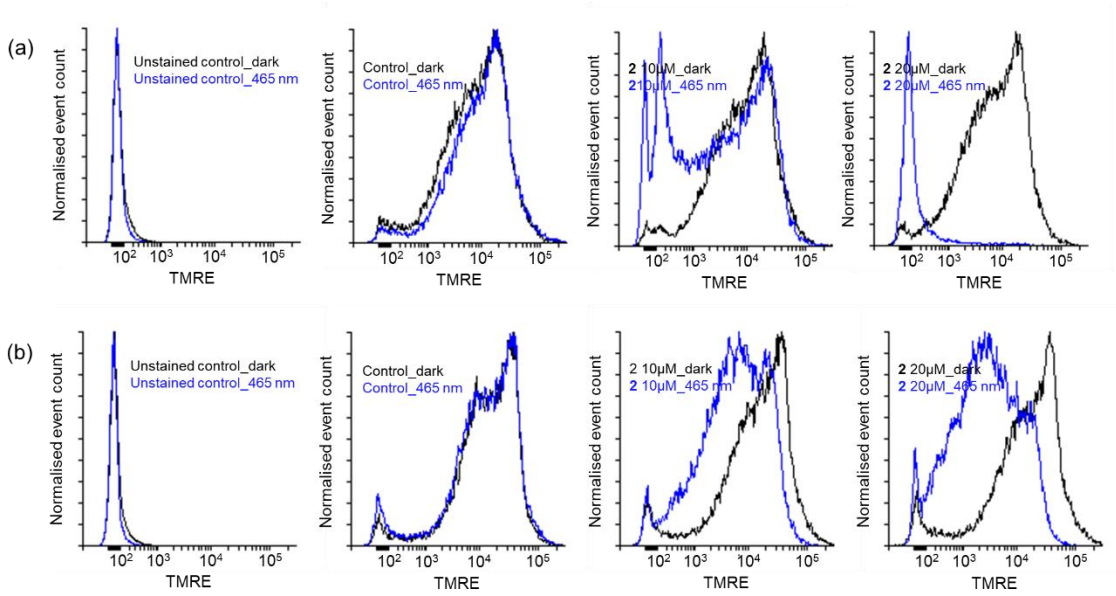

Figure S34. Mitochondrial potential of SW780 cells treated with **2** (0, 10 and 20 μM) in the dark (26 h) or 1 h incubation and 1 h irradiation (465 nm) and 24 h further incubation without drug removal under (a) normoxia or (b) hypoxia, then stained by TMRE ($\lambda_{ex}/\lambda_{em}$ = 561/570−600 nm) and analysed by flow cytometry.

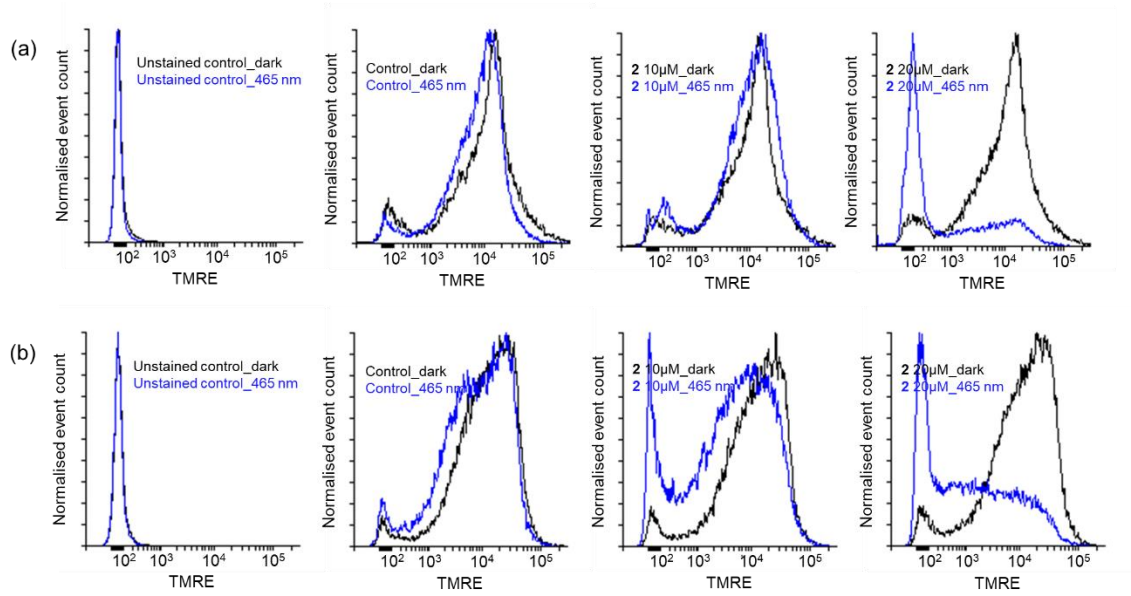

Figure S35. Mitochondrial potential of SW780 cells treated with **2** (0, 10 and 20 μM) in the dark (74 h) or 1 h incubation and 1 h irradiation (465 n) and 72 h further incubation without drug removal under (a) normoxia or (b) hypoxia, then stained by TMRE ($\lambda_{ex}/\lambda_{em}$ = 561/570−600 nm) and analysed by flow cytometry.

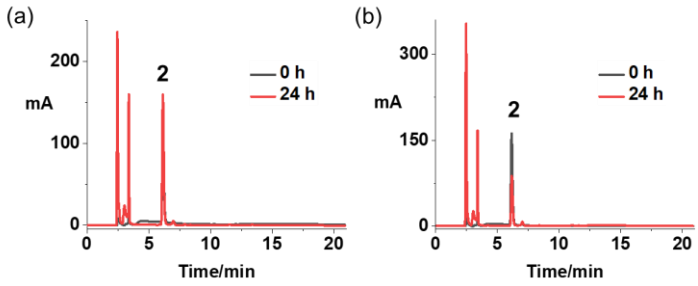

Figure S36. Dark stability of **2** for 24 h at 310 K (a in air-saturated PBS; b in N_2-saturated PBS) of 100 μM complexes in the presence of liver microsomes (0.25 mg/mL) and NADPH (100 μM) determined by HPLC.

References

1. O. V. Dolomanov, L. J. Bourhis, R. J. Gildea, J. A. K. Howard, H. Puschmann, *J. Appl. Crystallogr*., 2009, **42**, 339−341.
2. G. M. Sheldrick, *Acta Crystallogr*., Sect. A: Found. Adv., 2015, **71**, 3−8.
3. G. M. Sheldrick, *Acta Crystallogr., Sect. C: Struct. Chem*., 2015, **71**, 3−8.
4. V. Vichai, K. Kirtikara, *Nat. Protoc*., 2006, **1**, 1112−1116.
5. N. J. Farrer, J. A. Woods, L. Salassa, Y. Zhao, K. S. Robinson, G. Clarkson, F. S. MacKay and P. J. Sadler, *Angew. Chem. Int. Ed.*, 2010, **49**, 8905–8908.
6. H. Shi, F. Ponte, J. S. Grewal, G. J. Clarkson, C. Imberti, I. Hands-Portman, R. Dallmann, E. Sicilia and P. J. Sadler, *Chem. Sci.*, 2024, **15**, 4121–4134.